

## Review of phosphate removal from water by carbonaceous sorbents

Ismail W. Almanassra, Viktor Kochkodan, Gordon Mckay, Muataz Ali Atieh, Tareq Al-Ansari

### Item type

Journal Contribution

### Terms of use

This work is licensed under a [CC BY 4.0](https://creativecommons.org/licenses/by/4.0/) license

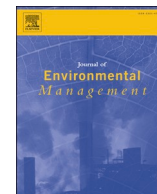
### This version is available at

[https://manara.qnl.qa/articles/journal\\_contribution/Review\\_of\\_phosphate\\_removal\\_from\\_water\\_by\\_carbonaceous\\_sorbents/2408/](https://manara.qnl.qa/articles/journal_contribution/Review_of_phosphate_removal_from_water_by_carbonaceous_sorbents/2408/)

Access the item on Manara for more information about usage details and recommended citation.

Posted on Manara – Qatar Research Repository on

2021-06-01



## Review

## Review of phosphate removal from water by carbonaceous sorbents

Ismail W. Almanassra<sup>a</sup>, Viktor Kochkodan<sup>b,\*,\*\*</sup>, Gordon McKay<sup>a</sup>, Muataz Ali Atieh<sup>c,d</sup>,  
Tareq Al-Ansari<sup>a,e,\*</sup>

<sup>a</sup> Division of Sustainable Development, College of Science and Engineering, Hamad Bin Khalifa University, Qatar Foundation, Doha, Qatar

<sup>b</sup> Qatar Environment and Energy Research Institute, Hamad Bin Khalifa University, Qatar Foundation, PO Box 5825, Doha, Qatar

<sup>c</sup> College of Engineering, University of Sharjah, PO Box 27272, Sharjah, United Arab Emirates

<sup>d</sup> Desalination Research Group, Research Institute of Sciences and Engineering, University of Sharjah, PO Box 27272, Sharjah, United Arab Emirates

<sup>e</sup> Division of Engineering Management and Decision Sciences, College of Science and Engineering, Hamad Bin Khalifa University, Qatar Foundation, Doha, Qatar

## ARTICLE INFO

## Keywords:

Phosphate  
Adsorption  
Activated carbon  
Graphene  
CNTs  
Water treatment

## ABSTRACT

In the last decades, phosphate is considered the main cause of eutrophication and has received substantial attention from the scientific community. Phosphate is a major pollutant that deteriorates water quality, which has been increasing in water resources, primarily due to the increasing global population and corresponding activities. Adsorption technology is amongst the different technologies used to decrease the phosphate levels in water, and has been found to be highly effective even at low phosphate concentrations. Carbonaceous materials and their composites have been widely used for phosphate removal due to their exceptional surface properties and high phosphate sorption capacity. Considering the importance of the topic, this study reviews the reported literature in the field of adsorptive removal of phosphate over various carbon-based adsorbents such as activated carbon, charcoal, graphene, graphene oxide, graphite and carbon nanotubes. Moreover, insights into the adsorption behaviour, experimental parameters, mechanisms, thermodynamics, effect of coexisting ions and the possible desorption processes of phosphate onto modified and unmodified carbonaceous adsorbents are also considered. Finally, research challenges and gaps have been highlighted.

## 1. Introduction

The continuous discharge of pollutants into aquatic environments is leading to the deterioration in the quality of water resources (Kumwimba et al., 2020). There has been a growing presence of phosphates in water resources over the years from various sources, where the two most problematic sources are: (i) the run-off from farmland agricultural areas as a result of land-spreading of phosphate fertilisers, and their subsequent dissolution into rainwaters with their consequent disperse discharge into streams and rivers; (ii) their presence in sewage streams and their subsequent presence after treatment in the sewage sludge treatment plants and in the treated sewage effluent (TSE) (Dai et al., 2021). The problem of phosphates in agricultural land run-off has manifested itself in excessive algal growth in streams and rivers, and most significantly their migration into reservoirs to such an extent that water pipelines and turbines have resulted in blockages (Irwin et al., 2018). Further extensive economic disruptions have been caused by the

appearance of the dinoflagellates, toxic red algae, in the shore line seawaters wiping out millions of dollars' worth of fish farming stocks (Haley et al., 2017; Quimpo et al., 2020). In the last ten years, a significant amount of research has been initiated in the use of TSE for agricultural applications, attributed largely to the food security challenges and water stress and scarcity in many countries, and of course, the presence of the plant nutrient phosphate (Kumwimba et al., 2020; Vikrant et al., 2017; Zhi et al., 2020). To fertilise land using "phosphate waste", whether from farmland run-off or from TSE, can contribute towards recover, recycle and re-use objectives within the global sustainable development agenda. However, in the case of the direct application of TSE water; there is a challenge related to the varying concentrations of TSE, where the applied phosphate dosing on the land may not be consistent. Consequently, the removal of phosphate by adsorption prior to further recovery and re-use is of benefit in order to control the application of the recovered phosphate (Nakarmi et al., 2020; Novais et al., 2018). The phosphate can be desorbed off the adsorbent providing

**Abbreviations:** PFO, Pseudo first order; PSO, Pseudo second order; L, Langmuir; F, Freundlich; L-F, Langmuir-Freundlich;  $Q_m$ , maximum adsorption capacity.

\* Corresponding author. P.O. Box: 34110, Doha, Qatar.

\*\* Corresponding author. P.O. Box: 34110, Doha, Qatar.

E-mail addresses: [vkochkodan@hbku.edu.qa](mailto:vkochkodan@hbku.edu.qa) (V. Kochkodan), [talansari@hbku.edu.qa](mailto:talansari@hbku.edu.qa) (T. Al-Ansari).

<https://doi.org/10.1016/j.jenvman.2021.112245>

Received 11 November 2020; Received in revised form 5 January 2021; Accepted 20 February 2021

Available online 15 March 2021

0301-4797/© 2021 The Author(s). Published by Elsevier Ltd. This is an open access article under the CC BY license (<http://creativecommons.org/licenses/by/4.0/>).

a phosphate liquid fertiliser, the concentration of which can be adjusted to a fixed design value. The adsorbent can then be reused in further adsorption applications.

Essentially, the phosphate remediation from aqueous solutions is usually achieved by biological, physical or chemical processes. Table 1 lists the advantages and disadvantages of the main conventional technologies used for the removal of phosphate from water and wastewater effluents. Amongst these technologies, is the adsorption process, which is considered effective at low phosphate concentration, easy and cheap in its plant operation, supports the possibility of using low cost adsorbents and provides the ability of phosphate recovery after adsorption (Bacelo et al., 2020; Ghorbani et al., 2020; Almanassra et al., 2020a; Lin et al., 2016; Siyal et al., 2020).

Different adsorbents have been suggested for phosphate mediation from aqueous solutions, such as; activated carbon, graphene, zeolites, polymers, metal oxides/hydroxides and porous silica. In particular, carbonaceous materials and their composites have been widely utilised due to their exceptional properties, such as large specific surface area, abundant pore structure, chemical stability, ease of physical and chemical modification, tunable properties for specific application and ability to remove a variety of pollutants (Qi et al., 2014; Xiong et al., 2018). Fig. 1 illustrates the bibliographic data of phosphate removal by carbonaceous materials (activated carbon, graphite, carbon nanotubes, graphene, graphene oxide, charcoal and others). The use of carbonaceous materials is rapidly growing for the capture of different pollutants, and hence several reviews have studied pollutant capture by carbonaceous materials (Ghorbani et al., 2020; Smith and Rodrigues, 2015; Suresh and Bandosz, 2018; Xiang et al., 2019). As such, there is a need to provide the readers and the wider scientific community with a holistic review of phosphate removal by carbon based adsorbents.

**Table 1**

Advantages and disadvantages of the main technologies used for phosphate removal from wastewater.

Process	Advantages	Disadvantages
Adsorption	<ul style="list-style-type: none"> <li>• Easy process operation.</li> <li>• Effective at low phosphate concentrations.</li> <li>• Low initial cost.</li> <li>• Low amount of by-products.</li> <li>• Fast process.</li> <li>• Adsorbed phosphate could be recovered (Ghorbani et al., 2020; Lin et al., 2016; Siyal et al., 2020).</li> </ul>	<ul style="list-style-type: none"> <li>• Adsorbent regeneration requires additional cost.</li> <li>• The effect of co-existing ions, selectivity against other contaminants.</li> </ul>
Biological processes such as the conventional activated sludge treatment	<ul style="list-style-type: none"> <li>• Can achieve complete removal of phosphate.</li> <li>• Low operation cost.</li> <li>• Low amount of by-products (Huang et al., 2017).</li> </ul>	<ul style="list-style-type: none"> <li>• Strict control of operational parameters is required (Loganathan et al., 2014).</li> <li>• Not effective in the removal of trace amounts of phosphate (Bacelo et al., 2020; Huang et al., 2017).</li> </ul>
Chemical precipitation using lime, calcium, magnesium, aluminum and iron salts	<ul style="list-style-type: none"> <li>• Well established process.</li> <li>• Reliable process.</li> <li>• Can achieve high phosphate removal (Kyong et al., 2014).</li> </ul>	<ul style="list-style-type: none"> <li>• Requires continuous effluent neutralization.</li> <li>• High chemical consumption.</li> <li>• Sludge disposal.</li> <li>• Not effective at low phosphate concentrations (Loganathan et al., 2014).</li> </ul>
Physical processes such as reverse osmosis and electrodialysis	<ul style="list-style-type: none"> <li>• High phosphate removal.</li> </ul>	<ul style="list-style-type: none"> <li>• High capital, energy and operational costs.</li> <li>• Poor selectivity of ions.</li> </ul>

Although several studies have been reported in the last decade which have reviewed phosphate removal by adsorption (Ahmed et al., 2019; Bacelo et al., 2020; Huang et al., 2017; Li et al., 2016; Liu et al., 2018; Almanassra et al., 2021; Loganathan et al., 2014; Zhi et al., 2020); to the best of our knowledge, there is no comprehensive review on the removal of phosphate by carbon based materials. With the exception of partial sections in certain reviews (Bacelo et al., 2020; Liu et al., 2018; Loganathan et al., 2014). Hereby, we have reviewed the most cited papers of phosphate removal by carbonaceous materials with more focus on the most recent publications in the last decade.

This study presents a comprehensive and critical review of the literature that reported the batch adsorptive phosphate removal by modified and unmodified carbonaceous materials namely; activated carbon, CNTs, graphene, graphene oxide, graphite, graphite oxide, charcoal, porous carbon, carbon nanofibers, mesoporous carbon (CMK-3) and carbide derived carbon. A summary of the published data in terms of: adsorbent preparation techniques; adsorbent surface properties; adsorption experimental conditions, isotherms; kinetics, optimum pH and maximum adsorption capacity are presented. The effect of coexisting ions, adsorption thermodynamics, desorption analysis and phosphate adsorption mechanisms are also discussed. Furthermore, the review conclusions and future prospects of the phosphate removal by carbonaceous materials are also highlighted.

## 2. Phosphate removal by carbonaceous adsorbents and their composites

### 2.1. Activated carbon based adsorbents

Activated carbon (AC) has been widely used for the removal of organic and inorganic pollutants due to its high surface area, low cost, availability and surface porosity (Yagub et al., 2014; Zare and Gupta, 2015). According to the application of the AC, it is produced in different forms, powdered activated carbon, granulated activated carbon and activated carbon fibres. The properties of the AC depend on the raw material source and the preparation/activation method. The AC can be produced from different carbon rich materials including nut shell, lignin, pine cone mass, coir pith and so on. However, most of the ACs possess a negatively charged functional groups onto their surfaces, and hence, the AC demonstrates low adsorption removal of the anionic pollutants such as phosphate (Bacelo et al., 2020). Phosphate removal by activated carbon began 30 years ago in 1990 by Ferro et al. (1990), who tested the AC produced from almond shell and olive stone produced by CO<sub>2</sub> activation. The produced ACs were of high surface area, however, with a limited phosphate adsorption capacity. As such, in the following decades, the ACs were either activated by other methods or impregnated by some materials, which demonstrate an affinity toward phosphate ions to improve the adsorption capacity of phosphates onto ACs. This section has been divided according to the origin of the AC, modified and un-modified commercial AC, the effect of the AC activation method produced from the different sources of biomass, phosphate removal by modified biomass derived AC, activated carbon fibre composites and granulated activated carbon composites.

#### 2.1.1. Phosphate removal by commercial AC

As received commercial AC was tested for phosphate removal by Mehrabi et al. (2016), who optimised the best conditions for phosphate removal from drinking water using the response surface methodology. It was concluded that the optimised conditions included an AC dose of 1.06 g/L, pH 4 and initial concentration of phosphate of 11.62 ppm, whilst the commercial AC of surface area of 922 m<sup>2</sup>/g can achieve a 95.41% removal of phosphate from drinking water. To enhance the removal of phosphate by commercial AC, Al-zboon (2018) determined that the addition of 15 wt% of silica onto the AC improved the phosphate removal from water. However, this adsorbent demonstrated one of the lowest reported adsorption capacities of phosphate of 0.645 mg

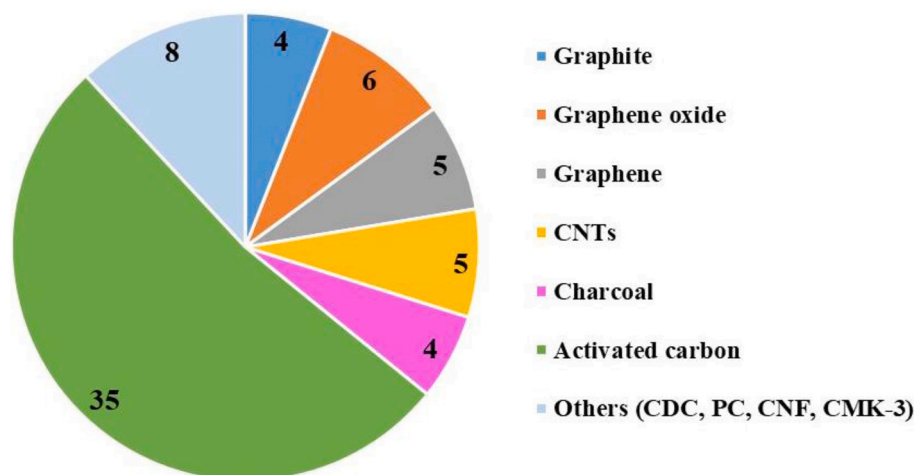


Fig. 1. Statistics of the number of the reviewed papers of phosphate removal by carbonaceous materials.

( $\text{PO}_4^{3-}$ )/g.

Modifying the commercial AC with iron and magnesium was found to significantly improve the adsorption capacity of phosphate (Shi et al., 2011; Wang et al., 2012, 2014; Zhu et al., 2018). Shi et al. (2011) treated the commercial AC with nitric acid followed by loading with iron oxide (AC-Fe(III)O). The study determined that the optimised iron content onto the AC was 15.05 mg/g. The surface properties decreased after iron loading due to the surface coverage and pore blockage by the iron nanoparticles, decreasing from 1039 to 668.2  $\text{m}^2/\text{g}$ , whilst the average pore diameter decreased from 1.869 to 1.692 nm. The maximum adsorption capacity was 98.39 and 78.9  $\text{mg}(\text{PO}_4^{3-})/\text{g}$  for AC-Fe(III)O and acid treated AC, respectively. Fig. 2 illustrates the isotherm and kinetics of phosphate uptake onto these ACs, the high adsorption capacity of the used ACs attributed to the oxidation of AC by nitric acid, in addition to increasing the number of adsorption sites by iron oxide doping. Iron, divalent and trivalent, was loaded onto the oxidised AC by Wang et al. (2012), which were firstly oxidised by  $\text{HNO}_3$  (AC/N), then functionalised with ferric sulphate and ferric chloride to prepare the AC/NFe<sup>III</sup> and AC/NFe<sup>II</sup>, respectively. After functionalisation; AC/NFe<sup>II</sup> has a significantly higher surface area than AC/NFe<sup>III</sup> because Fe<sup>III</sup> form large particle clusters that cannot diffuse into the internal pores of the AC, although they precipitate onto the macro-pores and coat the external surface of the AC. Both adsorbents reached equilibrium in 240 min and the highest phosphate removal was in the pH range of 3.78–6.84. The maximum adsorption capacities were 14.12 and 8.73  $\text{mg}(\text{PO}_4^{3-})/\text{g}$  for AC/NFe<sup>II</sup> and AC/NFe<sup>III</sup>, respectively. The higher adsorption capacity of AC/NFe<sup>II</sup> was attributed to its better intra-particle diffusion and higher binding energy. Wang et al. (2014) studied

phosphate remediation by oxidising an un-oxidised AC impregnated with iron oxide named as OAC/Fe and AC/Fe, respectively. The OAC demonstrated a higher affinity to adsorb Fe ions than the un-oxidised AC, where the iron content was 7.56% and 4.03% for the OAC and un-oxidised AC, respectively. The highest phosphate adsorption capacity was 15.87 and 8.47  $\text{mg}(\text{PO}_4^{3-})/\text{g}$  for the OAC/Fe and AC/Fe, respectively. The higher adsorption capacity of OAC/Fe was attributed to better surface mass transfer, intra-particle diffusion and a higher binding energy than the AC/Fe. Zhu et al. (2018) modified the commercial AC with MgO. The ACs were activated by  $\text{CO}_2$  and  $\text{N}_2$  before impregnation to improve the porosity of the carbon material. The  $\text{N}_2$  activation demonstrated a lower adsorption capacity, because it has lower surface area and the lower dissolution of MgO particles in both the solution and the carbon matrix surface. The MgO-modified AC reported the highest adsorption capacity of phosphate onto the different modified ACs. The highest adsorption capacity was 294  $\text{mg}(\text{P})/\text{g}$  at 35 °C following the Langmuir adsorption isotherm model. This was attributed to: (i) the high affinity of phosphate ions toward the adsorbent surface; and (ii) the high point zero of charge (PZC) (12) of Mg particles, which significantly promoted the electrostatic interactions between the negatively charged phosphate ions and the positively charged adsorbent surface. Table 2 lists the literature of phosphate removal by commercial ACs.

#### 2.1.2. Effect of activation method of biomass derived AC on phosphate removal

As seen from Table S1, different activation methods have been used for AC production. For example, Ferro et al. (1990) used the  $\text{CO}_2$  activation at 840 °C to prepare ACs from almond shell and olive stone. The

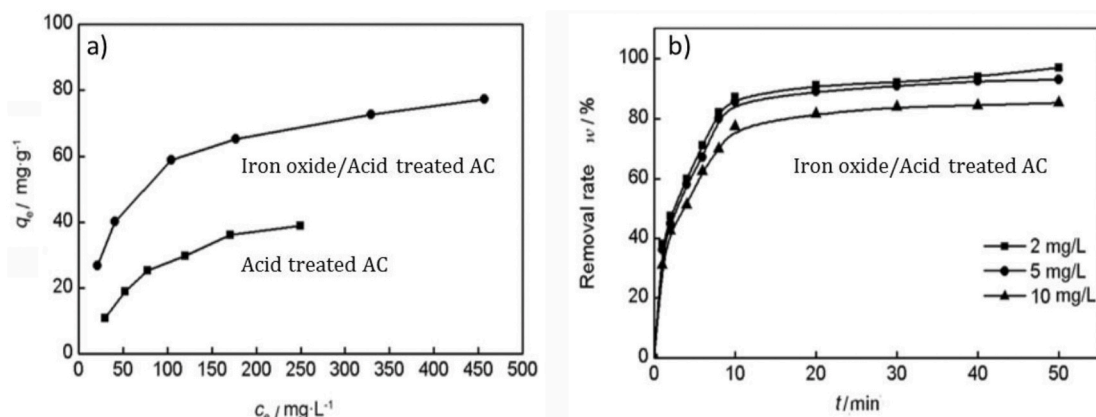


Fig. 2. Phosphate adsorption onto iron oxide doped acid treated AC, a) Isotherm, b) kinetics (Shi et al., 2011).

**Table 2**

Summary of the reported studies of phosphate removal by commercial AC.

Adsorbent	Adsorbent preparation technique	Studied phosphate concentration (mg/L)	Surface area (m <sup>2</sup> /g)	PZC	Qm (mg/g)	Kinetics	Isotherm	Adsorbent dose D (g/L), Optimum pH <sub>opt</sub> Equilibrium time (T)	Adsorption Mechanism	Ref
AC doped with Fe(III)O	Virgin AC modified by HNO <sub>3</sub> , then functionalised by iron nitrate.	200–1200 (PO <sub>4</sub> <sup>3-</sup> )	668.2	–	98.4 (PO <sub>4</sub> <sup>3-</sup> ) at pH 3	PSO	F	D: 0.8 pH <sub>opt</sub> : 2 T: 10 min	Ligand exchange	Shi et al. (2011)
AC/N–FeII	Commercial AC oxidised by HNO <sub>3</sub> to AC/N then functionalised by ferric sulphate or ferric chloride.	11.82–42.96 (PO <sub>4</sub> <sup>3-</sup> )	880.7	–	14.1 (PO <sub>4</sub> <sup>3-</sup> ) at 25 °C	PSO, Intra-particle diffusion	L	D: 2 pH <sub>opt</sub> : 3.78–6.84 T: 240 min	Chemisorption	Wang et al. (2012)
AC/N–FeIII			302.6	–	8.7 (PO <sub>4</sub> <sup>3-</sup> ) at 25 °C					
AC–MgO	AC produced by CO <sub>2</sub> activation of hydrochar at 700 °C for 2 h, MgO doping by functionalisation.	1–150 (P)	297	–	294 (P) at 35 °C	–	L	D: 0.5 pH <sub>opt</sub> : – T: –	Precipitation	Zhu et al. (2018)
Pre-oxidised AC impregnated with Fe	AC were oxidised by HNO <sub>3</sub> followed by Iron impregnation.	9.03–39.22 (PO <sub>4</sub> <sup>3-</sup> )	880.65	5.76	15.87 (PO <sub>4</sub> <sup>3-</sup> ) at 40 °C	PSO	L	D: 2 pH <sub>opt</sub> : – T: –	Electrostatic forces,	Wang et al. (2014)
AC impregnated with Fe	Impregnation of iron oxide.		1059.67	6.9	7.47 (PO <sub>4</sub> <sup>3-</sup> ) at 40 °C				Internal bonds	

surface area increased with activation time, where the highest surface area was 968 and 1030 m<sup>2</sup>/g after 30 h of activation for almond shells and olive stone ACs, respectively. The adsorption data following the Langmuir model with a maximum adsorption capacity of 4.9 and 4.4 mg (PO<sub>4</sub><sup>3-</sup>)/g for the almond shell and olive stone ACs, respectively. Although AC obtained from olive stone has higher surface area than the almond shell AC, it provides lower adsorption capacity because the surface the almond shell AC is less basic in nature than the olive stone AC. The authors determined that these manufactured ACs have higher adsorption capacities than the commercial AC. Kilpimaa et al. (2015) utilised the carbon residues from a biomass gasification process to prepare AC by physical activation. The study compares the surface properties and phosphate uptake of different activating agents CO<sub>2</sub>, CO and N<sub>2</sub>, under different activation temperature and activation periods. The highest surface area (590 m<sup>2</sup>/g) was obtained for the AC residues activated by CO<sub>2</sub> at an activation temperature of 800 °C for 3 h. The optimised adsorbent illustrates a maximum phosphate adsorption capacity of 30.21 mg(PO<sub>4</sub><sup>3-</sup>)/g. The authors concluded that the adsorption is related to the porosity of the adsorbent. Kilpimaa et al. (2014) also chemically activated the carbon residues by the wet impregnation method using HCl, H<sub>2</sub>SO<sub>4</sub>, ZnCl<sub>2</sub>, KOH and HNO<sub>3</sub>. The highest surface area of AC 285 m<sup>2</sup>/g was obtained when the feed stock treated by 5 M ZnCl<sub>2</sub> and activation temperature 500 °C for 1 h. The obtained AC has very fast kinetics toward phosphate ions and equilibrium was reached in 1 min compared to 24 h for AC obtained by CO<sub>2</sub> activation. Precipitation of phosphate ions by the zinc and calcium ions within the AC residues structure was the controlling mechanism of the adsorption process. Bhargava and Sheldarkar (1993) prepared AC from the tamarind nut shell (TNSAC). The obtained AC was first impregnated with ZnCl<sub>2</sub> then thermally activated at 700 °C for 1–2 h. The phosphate adsorption capacity of TNSAC was 29 mg/g, where the equilibrium was achieved in 100 min.

Coir pith has been used for AC production by chemical and thermal activation methods. For example, Namasivayam and Sangeetha (2004) obtained AC by chemically activating the coir pith using ZnCl<sub>2</sub> followed by carbonisation at 700 °C. The adsorbent demonstrated a maximum adsorption capacity of 5.1 mg(PO<sub>4</sub><sup>3-</sup>)/g and equilibrium was reached in 100 min. Kumar et al. (2010) utilised the chemical activation method by H<sub>2</sub>SO<sub>4</sub> followed by carbonisation at 600 °C for AC production from coir

pith. The adsorbent had a surface area of 727.4 m<sup>2</sup>/g with a positive charge over a wide range of pH due to a PZC of 9.9). The maximum phosphate adsorption capacity was 7.74 mg(PO<sub>4</sub><sup>3-</sup>)/g and the equilibrium was reached in 3 h. The AC obtained from coir pith demonstrated a stable adsorption capacity in the pH range 4–10. Similarly, Manjunath and Kumar (2018) utilised chemical treatment with sulfuric acid followed by thermal treatment at 500 °C. Xu et al. (2015) used H<sub>4</sub>P<sub>2</sub>O<sub>7</sub> as an activating agent for AC production from Arundo donax Linn. The feed stock was initially thermally treated at 400 °C followed by activation. The produced AC has a surface area and PZC of 1.34 m<sup>2</sup>/g and 4.2, respectively. The maximum phosphate adsorption capacity was 7.7 mg (PO<sub>4</sub><sup>3-</sup>)/g and the authors concluded that the adsorption process involved both physisorption and chemisorption mechanisms. A summary of the studies reporting phosphate removal by AC produced by different activation methods is presented in Table S1.

### 2.1.3. Modified biomass derived AC

The adsorption capacity of the AC produced from direct activation of natural materials can be improved by impregnation with different materials. For instance, Yao et al. (2018) impregnated the AC obtained from sewage sludge with 1 wt% of pyrolusite (pyrolusite is a natural material composed of metal oxides). The impregnation of AC with pyrolusite improved the surface area, pore volume and the average pore diameter of the AC. The maximum phosphate adsorption capacity was 2.78 and 10.78 mg(P)/g for the unmodified and impregnated ACs, respectively. Moreover, Han et al. (2020), fabricated a magnetic bio AC prepared from lignin. A novel streamlined preparation process was used for the adsorbent synthesis, where the carbonisation process was performed at 800 °C followed by steam treatment as illustrated in Fig. S1. The steam acts as an activating agent for pore generation, pore widening and assisting in the oxidation of iron species on the AC surface. The synthesised AC demonstrates a maximum phosphate adsorption capacity of 21.18 mg(PO<sub>4</sub><sup>3-</sup>)/g. Huong et al. (2019) reported phosphate removal by pine cone biomass AC modified with lanthanum. The La-modified AC has a surface area of 380 m<sup>2</sup>/g and a PZC of 7.2. The synthesised adsorbent demonstrates a maximum adsorption capacity of 68.2 mg (P)/g for phosphate. Furthermore, Karthikeyan and Meenakshi (2019) prepared an AC from banana waste functionalised with layered double hydroxides binary composite Zn and Al. The AC was initially prepared



by chemical activation using  $\text{H}_2\text{SO}_4$  then thermal carbonisation at  $400\text{ }^\circ\text{C}$  for 6 h. Finally, the metal hydroxides doping was accomplished by the co-precipitation method. The synthesised adsorbent demonstrates an adsorption capacity of  $87\text{ mg}(\text{PO}_4^{3-})/\text{g}$  and the equilibrium was achieved in 40 min. A summary of the reported studies of phosphate removal by modified biomass derived AC are presented in Table S2.

#### 2.1.4. Phosphate removal by activated carbon fibres

Activated carbon fibres (ACF) have been found to have a maximum phosphate sorption capacity of  $0.6\text{ mg(P)}/\text{g}$  (Zhou et al., 2012). The La and Fe ions were of significant interest for the modification of ACF to improve the sorption capacity of phosphate. Liu et al. (2011) and Zhang et al. (2011, 2012a, 2012b) modified the ACF with LaO by the impregnation method. The adsorbent demonstrated a PZC of 8.5 and the best phosphate removal was achieved at pH 4. The highest adsorption capacity was  $7.42\text{ mg(P)}/\text{g}$  at  $30\text{ }^\circ\text{C}$  in which inner and outer sphere complexes were occurring between phosphate ions and the adsorbent surface as illustrated in Fig. 3. The same research group has reported the phosphate removal by ACF modified with LaOH (Zhang et al., 2012b). The fabricated adsorbent illustrates a PZC of 8 and a maximum phosphate adsorption capacity of  $15.3\text{ mg(P)}/\text{g}$ . Zhang et al. (2012b) stated that at the same conditions, ACF-LaOH has a phosphate adsorption capacity of 46.4% greater than ACF-LaO, which was attributed to the fact that ACF-LaOH can offer more adsorption sites than ACF-LaO because of the replacement of the hydroxide groups in the former. Zhou et al. (2012) doped the same ACF used in the mentioned studies with hydrated ferric oxide nanoparticles (ACF-HFO) by the sol-gel method. Phosphate adsorption onto ACF-HFO has slow kinetics where equilibrium was reached in over 20 h. The maximum adsorption capacity of phosphate onto ACF-HFO is  $12.86\text{ mg(P)}/\text{g}$ .

In order to develop a cost-effective adsorbent, Liu et al. (2013) then merged the effect of iron and lanthanum. In this regard; Liu et al. (2013) reported phosphate removal using hydroxyl iron lanthanum ACF (ACF-LaFeOH). The adsorbent prepared by the modified proprietary synthetic process method developed by Solmetex. The adsorbent demonstrates a maximum phosphate adsorption capacity of  $29.44\text{ mg(P)}/\text{g}$ .

Moreover, the ACF-LaFeOH demonstrates faster kinetics (equilibrium was reached in 120 min) than ACF-HFO and ACF-LaOH. The binding affinity between ACF and iron lanthanum hydroxide was relatively weak as concluded by the authors. As such, Zhang et al. (2016a,b,c,d) prepared ACF impregnated with iron lanthanum oxides (ACF-LaFeO), which has better stability than the ACF-LaFeOH. The ACF-LaFeO has a PZC of 9.4, which is higher than that for ACF-LaFeOH (PZC is 8.5). There was no isotherm study for this adsorbent, however, the authors found that pH 4 is the optimum pH for the removal of phosphate by ACF-LaFeO.

Xiong et al. (2017) investigated the effect of iron and zirconium simultaneous functionalisation onto ACF (ACF-ZrFe). The adsorbent demonstrated a maximum phosphate adsorption capacity of  $26.3\text{ mg}(\text{PO}_4^{3-})/\text{g}$  and equilibrium was reached in 6 h. In another study, Sakamoto et al. (2020) utilised the polyacrylonitrile fibres to manufacture ACF by the chemical activation method using  $\text{K}_2\text{CO}_3$  at  $950\text{ }^\circ\text{C}$ . It was found that the ratio 3:1 of  $\text{K}_2\text{CO}_3$  to polyacrylonitrile mass ratio was the optimum in terms of phosphate uptake. Table S3 presents the literature of phosphate removal by ACF.

#### 2.1.5. Phosphate removal by granular activated carbon

Several studies have reported the phosphate removal by iron and lanthanum modified granular activated carbon (GAC). The commercial GAC demonstrated an adsorption capacity of  $9.35\text{ mg}(\text{PO}_4^{3-})/\text{g}$  from mineralised ground water, where the adsorption process is dominated by the Ca ions present in the groundwater solution (Ouakouak et al., 2017). The pre-oxidation process of GAC, before doping the metal nanoparticles assists in the fixation of Fe/La ions onto the surface of the GAC and this improved the adsorption capacity for phosphate. For example, Zach-maor et al. (2011) investigated the removal of phosphate using iron oxide impregnated GAC (nFe-GAC). The surface area of GAC was increased with iron oxide impregnation ( $866$  and  $1024\text{ m}^2/\text{g}$  for oxidised GAC and the pre-oxidised nFe-GAC, respectively), while the PZC reduced from 9.2 to 6.9 after impregnation. The oxidised GAC demonstrates negligible adsorption of phosphate, while the impregnated nFe-GAC uptake was  $435\text{ mg}(\text{PO}_4)/\text{g}(\text{Fe})$ . The adsorption process of

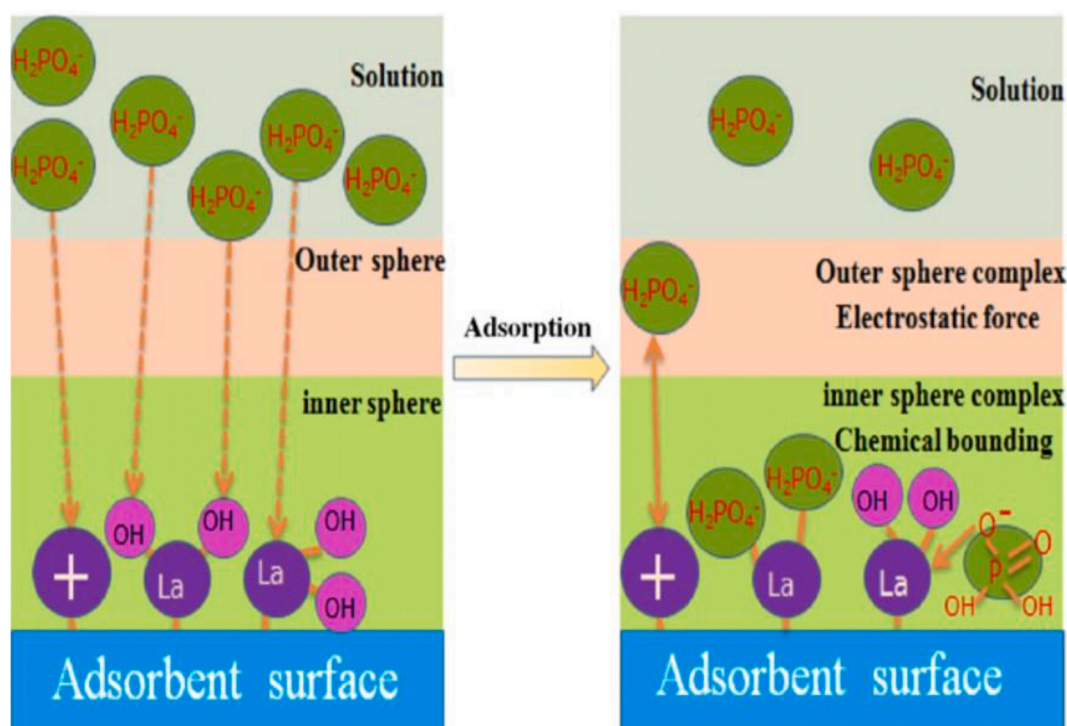


Fig. 3. Adsorption mechanisms of phosphate onto LaO-modified ACF (Zhang et al., 2011).

phosphate by nFe-GAC was controlled by the intraparticle diffusion process and followed the pseudo 2nd order model kinetics. Kumar et al. (2017) investigated the effect of the peroxidation on GAC functionalised with iron (GAC-Fe). The  $\text{KMnO}_4$  illustrates the maximum iron loading onto GAC and the maximum iron to oxygen molar ratio among other oxidising agents. Characterisation analysis explains that both iron nanoparticles and the adsorbed phosphate ions occurred in the mesopores and macropores, the internal micropores did not contribute to the adsorption process. Mahardika et al. (2018) reported phosphate removal by pre-oxidised GAC impregnated with amorphous ferrihydrite (FH@GAC). The pre-oxidation by the acid mixture  $\text{HNO}_3/\text{H}_2\text{SO}_4$  performed better in the creation of the functional groups in comparison with  $\text{NaOCl}$ , which in turn improved iron loading onto GAC. This is because  $\text{NaOCl}$  forms the C-Cl bond, which interferes with the binding of ferric ions with carbon. Braun et al. (2019) impregnated the surface of GAC with Fe without oxidation. The fabricated adsorbent was found to be unchanged in the pH range of (3.5–7) with a surface area of  $442.2 \text{ m}^2/\text{g}$ . The maximum adsorption capacity was  $2.87 \text{ mg}(\text{PO}_4^{3-})/\text{g}$  with very slow kinetics (equilibrium was reached in 75 h). The equilibrium data complies with the two sites Langmuir isotherm model.

Makita et al. (2019) investigated the GAC loaded by different metal oxides (lanthanum, iron and cerium oxides). It was found that lanthanum and cerium oxides loaded onto the GAC have a promising adsorption capability toward phosphate ions compared to iron oxide. The maximum adsorption capacity was 14.2 and 9.7  $\text{mg}(\text{P})/\text{g}$  for La-GAC and Ce-GAC, respectively. Khalil et al. (2017) studied the removal of phosphate by nano-zero-valent iron doped GAC (nZVI/GAC). The adsorbent has a high affinity toward phosphate ions and can achieve a complete removal of phosphate ions from their aqueous solutions with an initial phosphate concentration of 50 ppm using 5 g/L of the adsorbent. A summary of phosphate removal by GAC is presented in Table S4.

To conclude this section covering ACs, owing to their availability, ease of fabrication, high surface area; ACs were often more widely used than other carbon forms (graphene, carbon nanotubes and graphite). Due to the variety of experimental parameters, it is not easy to provide a proper comparison between the modifying elements, however, MgO-modified AC has demonstrated the highest ever reported adsorption capacity of phosphate onto the modified AC adsorbents (Zhu et al., 2018).

## 2.2. Graphene based adsorbents

Graphene is a single layer of graphitic carbon atoms that has a 2-D structure (Ibrahim et al., 2016). It has attracted much scientific attention due to its unique properties, such as low density, large specific surface area, can be uniformly distributed in water, a stable structure and a highly flexible material (Minale et al., 2020; Zhang et al., 2014). Moreover, graphene can be easily modified with different materials and this makes it an exceptional and promising adsorbent. Graphene and modified graphene have been utilised for the elimination of phosphate from the aqueous solutions in 5 reported articles between 2012 and 2017.

Raw graphene produced from natural graphite flakes by the facile liquid phase exfoliation technique has been tested for phosphate removal from water by Vasudevan and Lakshmi (2012). The results indicate that the obtained graphene sheets have a thickness of 2.98 nm with a PZC of 5.1. Graphene was found to demonstrate a stable adsorption capacity of  $13.21 \text{ mg}(\text{PO}_4^{3-})/\text{g}$  within the pH range 6–9. The obtained graphene also has comparable fast kinetics in which the equilibrium was reached in 10 min. Although simple prepared graphene has a higher phosphate adsorption capacity than the un-modified AC, the modification of graphene is of significant interest to enhance the phosphate adsorption capacity and decrease the release of graphene particulates into water (Nodeh et al., 2017; Tran et al., 2015).

To improve the adsorptive properties of phosphate, Graphene has been modified with lanthanum and iron oxides/hydroxides. For

instance, Zhang et al. (2014) proposed the modification of graphene nanosheets with  $\text{La}(\text{OH})_3$ , which led to the increase of the adsorbent charge from negatively charged to a PZC of 9.49. The modified graphene nanosheets show a maximum adsorption capacity of  $41.96 \text{ mg}(\text{P})/\text{g}$  in a period of 10 h; while it was  $0.17 \text{ mg}(\text{P})/\text{g}$  for the unmodified graphene. Chen et al. (2016), in their turn, suggested the use of  $\text{La}_2\text{O}_3$ .  $\text{La}_2\text{O}_3$ -modified graphene has a PZC of 5 and shows a maximum adsorption capacity of  $82.6 \text{ mg}(\text{PO}_4^{3-})/\text{g}$ . The saturation capacity has been reached in 25 min for an initial phosphate concentration of 142  $\text{mg}/\text{L}$ .

The incorporation of iron oxides/hydroxides have shown to enhance the adsorption properties of graphene (Nodeh et al., 2017; Tran et al., 2015). For example, Tran et al. (2015) doped the surface of graphene with two types of iron oxide aerogels; goethite ( $\alpha\text{-FeOOH}$ ) and magnetite ( $\text{Fe}_3\text{O}_4$ ). Both the iron derivatives were doped on the surface of graphene by the reduction of graphene oxide using iron sulphate. Graphene- $\alpha\text{-FeOOH}$  was synthesised at a pH of 3–3.5 (hydrolysis), while graphene- $\text{Fe}_3\text{O}_4$  was treated at a pH 11 (co-precipitation). The prepared composites exhibited superior capabilities to adsorb phosphate from water at a wide range of pH especially in acidic media and reached equilibrium within 1 h. The isotherms followed the Freundlich model with a maximum adsorption capacity of 352 and 311  $\text{mg}(\text{PO}_4^{3-})/\text{g}$  for graphene- $\alpha\text{-FeOOH}$  and graphene- $\text{Fe}_3\text{O}_4$  respectively, as seen in Fig. 4. The authors attributed the difference in the adsorption capacity to the surface area of the prepared composites. Nodeh et al. (2017) synthesised magnetic graphene functionalised with  $\text{La}(\text{OH})_3$  adsorbent. Ferric chloride was used to obtain the magnetic graphene oxide before reducing the complex to magnetic graphene and finally lanthanum impregnation was applied. The modification procedure is described in Fig. S2. The adsorbent illustrates fast kinetics for phosphate removal (equilibrium time was 10 min) with an adsorption capacity of 116.28  $\text{mg}(\text{PO}_4^{3-})/\text{g}$ . Graphene based adsorbents are new materials and there are only a limited number of studies, noting that these materials are attractive because of their high surface area and ease of modification. A summary of the applications of phosphate removal by graphene-based adsorbents are presented in Table 3.

## 2.3. Graphene oxide based adsorbents

Graphene oxide (GO) is produced from the inexpensive and non-toxic graphite (Sakulpaisan et al., 2016). It has attracted widespread attention due to the presence of oxygen containing functional groups, such as carbonyl, carboxylic and hydroxyl onto the carbon layer edges (Lingamdinne et al., 2019; Zhao et al., 2014). The existence of these functional groups enhance the formation of metal cation complexes, which in turn will improve their affinity toward the removal of anionic contaminants like phosphate (Dikin et al., 2007). The reduced graphene oxide (rGO) is obtained by eliminating part of the oxygen functional groups on the GO surface and is generally produced by the chemical or thermal reduction of GO (Xiang et al., 2019). Both GO, rGO and their modified composites were tested for phosphate removal in 2016 by Sakulpaisan et al. (2016) and Luo et al. (2016). Graphene oxide and rGO generally demonstrated low phosphate adsorption capacity because they are rich in negative ions, which in turn will repel the phosphate ions rather than attracting them. For example, the maximum phosphate adsorption capacity by GO was 1.68  $\text{mg}/\text{g}$  in simulated wastewater (Sakulpaisan et al., 2016), while it was 7.42  $\text{mg}/\text{g}$  in deionised water for rGO (Luo et al., 2016). However, these numbers were significantly enhanced by the modification of GO with metals, since this modification turns the negative charge on GO and rGO to positively charged adsorbent species, which leads to enhancing the electrostatic interactions mechanism (Bai et al., 2018; Harijan and Chandra, 2017; Sakulpaisan et al., 2016).

Bai et al. (2018) decorated the GO with  $\alpha\text{-Fe}_2\text{O}_3$  using ferric chloride as a source of iron. The obtained composite was able to provide rapid kinetics for phosphate removal, where equilibrium was reached in 5 min with a maximum adsorption capacity of 93.28  $\text{mg}(\text{PO}_4^{3-})/\text{g}$ . The

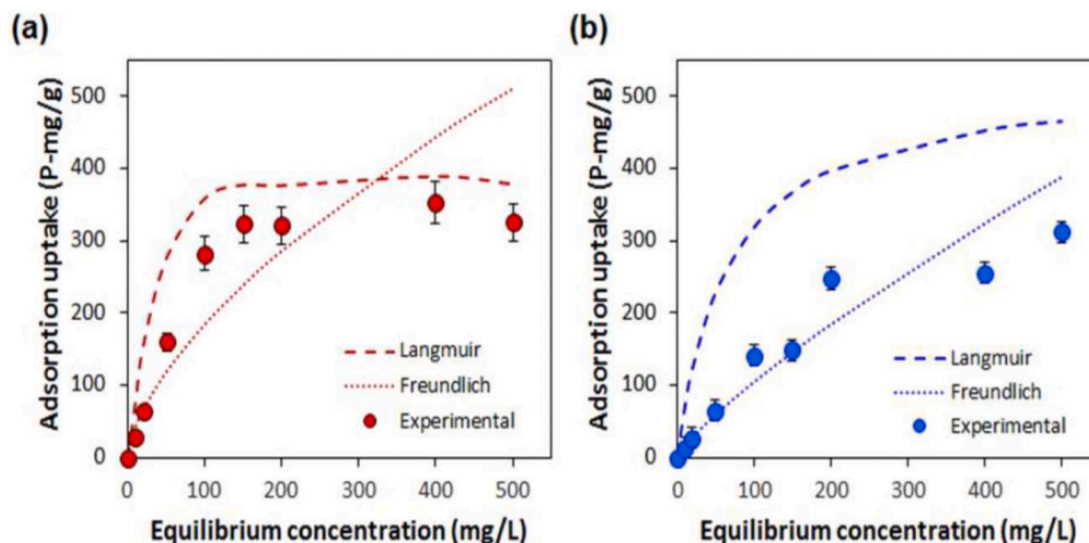


Fig. 4. Adsorption isotherm of phosphate removal by a) goethite ( $\alpha$ -FeOOH) modified graphene, b) magnetite ( $\text{Fe}_3\text{O}_4$ ) modified graphene (Tran et al., 2015).

Table 3

Summary of the reported studies of phosphate removal by graphene-based adsorbents.

Adsorbent	Adsorbent synthesis method	Studied phosphate concentration (mg/L)	PZC	$Q_m$ (mg/g)	Kinetics	Isotherm	Adsorbent dose D (g/L), Optimum pH, Equilibrium time (T)	Adsorption Mechanism	Ref
Graphene	Facile liquid phase exfoliation of graphite flakes	25–125 ( $\text{PO}_4^{3-}$ )	5.1	13.21 ( $\text{PO}_4^{3-}$ ) at pH 7, 30 °C	PSO	L	D: 0.66 pH <sub>opt</sub> : 6–8 T: 10 min	Ligand exchange	Vasudevan and Lakshmi (2012)
Graphene nanosheets supported lanthanum hydroxide	LaOH doping by microwave-assisted hydrothermal technique	10–60 (P)	9.49	41.96 (P) at 25 °C	PSO, Intra particle diffusion	L	D: 0.5 pH <sub>opt</sub> : 4 T: 10 h	Ligand exchange, Electrostatic and Lewis acid–base interactions	Zhang et al. (2014)
3 D graphene decorated lanthanum oxide	Hydrothermal reduction to produce 3D graphene– $\text{La}_2\text{O}_3$	14–292 ( $\text{PO}_4^{3-}$ )	5	82.6 ( $\text{PO}_4^{3-}$ ) at pH 6.2	PSO	L	D: 2 pH <sub>opt</sub> : 3–9 T: 25 min for 142 ppm	Ion exchange, Electrostatic interactions	Chen et al. (2016)
Graphene decorated with goethite ( $\alpha$ -FeOOH)	Reduction process at pH of 3–3.5 (hydrolysis)	10–500 ( $\text{PO}_4^{3-}$ )	–	352 ( $\text{PO}_4^{3-}$ ) at pH 6, 25 °C	PSO	F	D: 0.2 pH <sub>opt</sub> : 2 T: 1 h	Ligand exchange	Tran et al. (2015)
Graphene decorated with magnetite ( $\text{Fe}_3\text{O}_4$ )	Reduction process at pH 11 (co-precipitation)	–	–	311 ( $\text{PO}_4^{3-}$ ) at pH 6, 25 °C	–	–	–	–	–
Magnetic graphene loaded by lanthanum hydroxide	Impregnation process for lanthanum doping	10–200 ( $\text{PO}_4^{3-}$ )	–	116.28 ( $\text{PO}_4^{3-}$ ) at pH 6–8, 25 °C	PSO	L	D: 0.1 pH <sub>opt</sub> : 5–7 T: 10 min	Electrostatic interactions, Ligand exchange, $\pi$ - $\pi$ interaction	Nodeh et al. (2017)

adsorption capacity of phosphate was stable in the studied pH range (2–10.5) as the  $\alpha$ - $\text{Fe}_2\text{O}_3$ -GO nanoparticles maintain a positive charge of (+14.15 to +3.52 mV) in this pH range. Sakulpaisan et al. (2016) investigated phosphate removal from simulated wastewater by titania (Ti) functionalised GO. The Ti modification was performed by the sol-gel method. Ti doping on the surface of GO has increased the surface area from 52.8  $\text{m}^2/\text{g}$  to 162.9  $\text{m}^2/\text{g}$ . The Ti functionalised GO demonstrates a maximum adsorption capacity of 33.11  $\text{mg}(\text{PO}_4^{3-})/\text{g}$  compared to 1.68  $\text{mg}(\text{PO}_4^{3-})/\text{g}$  for unmodified GO.

A couple of studies have reported the decoration of rGO with zirconium and iron oxide (Akram et al., 2019; Luo et al., 2016). For instance, Luo et al. (2016) prepared zirconium-loaded rGO adsorbent by a green and facile method known as the one-step hydrothermal method without

using any reagents. The surface area, pore volume and average pore size were significantly improved with zirconium functionalisation as follows; 251.1  $\text{m}^2/\text{g}$ , 0.28  $\text{cm}^3/\text{g}$  and 5.55 nm for the fabricated adsorbent, and 46  $\text{m}^2/\text{g}$ , 0.16  $\text{cm}^3/\text{g}$  and 1.41 nm for rGO, respectively. These improvements produced an increase in the adsorption capacity from 7.42 to 27.71  $\text{mg}(\text{PO}_4^{3-})/\text{g}$ . Furthermore, Akram et al. (2019) fabricated an ammonia treated rGO decorated with iron oxide nanocomposite ( $\text{Fe}_3\text{O}_4$ ) to enhance the compatibility, stability and magnetic properties of nitrogen doped rGO. The maximum adsorption capacities were 169.7 and 135.3  $\text{mg}(\text{PO}_4^{3-})/\text{g}$  for iron decorated and undecorated adsorbents, respectively. The high adsorption capacities were attributed to the electrostatic interactions between phosphate and the doped nitrogen functionalities as demonstrated in Fig. 5. The authors explained that



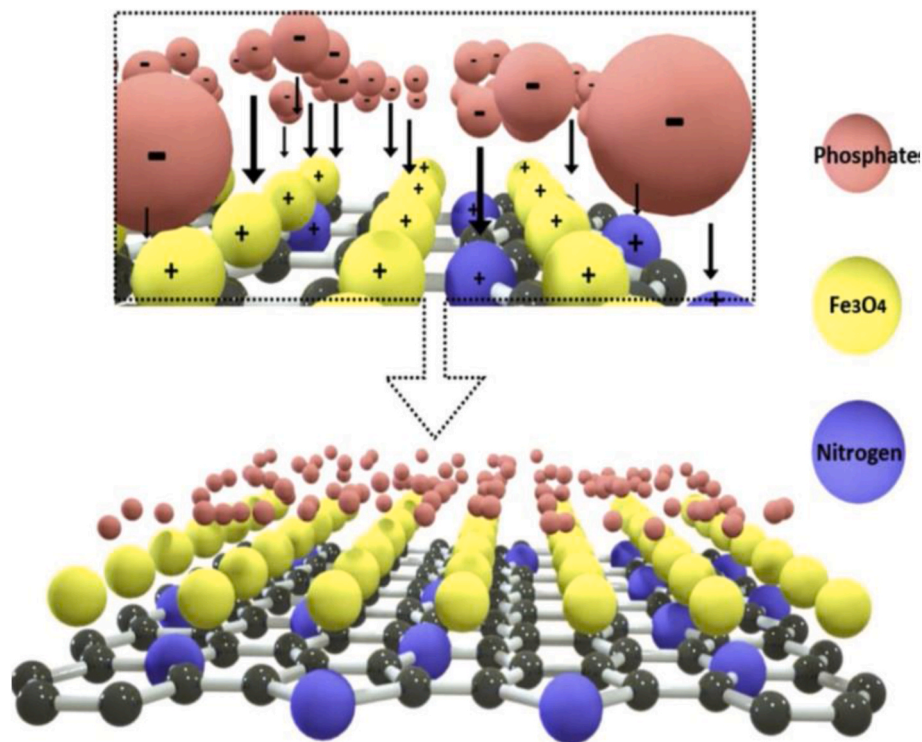


Fig. 5. The adsorption mechanism of phosphate onto nitrogen doped rGO decorated with iron oxide (Akram et al., 2019).

Table 4

Summary of the reported studies of phosphate removal by GO and rGO based adsorbents.

Adsorbent	Adsorbent synthesis method	Studied phosphate concentration (mg/L)	Surface area (m <sup>2</sup> /g)	$Q_m$ (mg/g)	Kinetics	Isotherm	Adsorbent dose D (g/L), Optimum pH, Equilibrium time (T)	Adsorption mechanism	Ref
GO	Modified Hummers' method	10–40 ( $\text{PO}_4^{3-}$ )	52.8	1.68 ( $\text{PO}_4^{3-}$ ) at pH 6, 25 °C, in stimulated wastewater	–	L	D: 1 pH <sub>opt</sub> : – T: 6 h	–	<a href="#">Sakulpaisan et al. (2016)</a>
Titania-functionalised GO	Sol-gel method		162.9	33.11 ( $\text{PO}_4^{3-}$ ) at pH 6, 25 °C	–	L	D: 1 pH <sub>opt</sub> : 2 T: 6 h	Electrostatic forces	
GO	Modified Hummers' method	0.1–5 ( $\text{PO}_4^{3-}$ )	46	7.42 ( $\text{PO}_4^{3-}$ ) at pH 5, 25 °C, in water.	PSO	L	D: 0.025–0.2 pH <sub>opt</sub> : – T: –	–	<a href="#">Luo et al. (2016)</a>
Zirconium-loaded rGO	One-step hydrothermal method		251.1	27.71 ( $\text{PO}_4^{3-}$ ) at pH 5, 25 °C.	PSO	L	D: 0.025–0.2 pH <sub>opt</sub> : 5 T: 375 min for 5 ppm PZC: 3.62	Electrostatic interactions.	
GO decorated with $\alpha\text{-Fe}_2\text{O}_3$	GO by modified hummers method and ferric chloride for decoration	10–150 ( $\text{PO}_4^{3-}$ )	–	93.28 ( $\text{PO}_4^{3-}$ ) at pH 6, 25 °C	PSO	L	D: 0.65 pH <sub>opt</sub> : 2–10 T: 5 min	Electrostatic attraction Ion exchange	<a href="#">Bai et al. (2018)</a>
Akaganeite ( $\beta\text{-FeOOH}$ ) nanorods decorated GO	GnO by hummers method, $\beta\text{-FeOOH}$ by hydrolysis and aging of anhydrous $\text{FeCl}_3$	5–30 ( $\text{PO}_4^{3-}$ )	80	45.2 ( $\text{PO}_4^{3-}$ ) at pH 7, 30 °C.	PSO	L	D: 0.4 pH <sub>opt</sub> : 3 T: 2 h	Columbic interactions Ligand exchange	<a href="#">Harijan and Chandra (2017)</a>
GO with the presence of 0.05 mM europium (III)	Modified hummers method	–	–	69.33 ( $\text{PO}_4^{3-}$ ) at pH 4, 20 °C, 0.01 M NaCl	PSO	L	D: 0.025 pH <sub>opt</sub> : 5.5–9 T: 2 h	Electrostatic attraction Surface complexation Precipitation	<a href="#">Xu et al. (2016)</a>
Nitrogen doped rGO	Solvo-thermal approach	5–50 ( $\text{PO}_4^{3-}$ )	–	135.3 ( $\text{PO}_4^{3-}$ ) at pH 5, 30 °C	PSO	F	D: 0.2 pH <sub>opt</sub> : 4 T: 6 h	Electrostatic interactions.	<a href="#">Akram et al. (2019)</a>
Nitrogen doped rGO decorated with $\text{Fe}_3\text{O}_4$	Polyol technique		–	169.7 ( $\text{PO}_4^{3-}$ ) at pH 5, 30 °C	PSO	F	D: 0.2 pH <sub>opt</sub> : 5 T: 6 h		

$\text{Fe}_3\text{O}_4$  decoration acts as a pillars and nanospacers, which enhances the stability and prevents the agglomeration of adsorbent particles, which is not the case of without iron decoration. Without iron decoration, the adsorbent particles were agglomerating, leading to loss of surface area and active adsorption sites.

The adsorption of phosphate was found to be promoted with the existence of europium (Eu III). Xu et al. (2016) reported that the existence of 0.05 mmol/L of Eu (III) in the phosphate solutions increases the adsorption capacity to 69.33  $\text{mg}(\text{PO}_4^{3-})/\text{g}$  compared to the negligible removal in the absence of europium (III). This was attributed to the addition of Eu (III) having increased the zeta potential values of GO, which makes it more attractive to phosphate ions.

Harijan and Chandra (2017) have used the GO decoration to enhance the stability of akaganeite ( $\beta\text{-FeOOH}$ ) nanoparticles against leaching out. The maximum phosphate removal was obtained at 5 wt% loading of GO onto akaganeite. This loading increased the aspect ratio of akaganeite from 5 to 7 and increased the BET surface area from 20 to 80  $\text{m}^2/\text{g}$  with a corresponding maximum phosphate adsorption capacity of 45.2  $\text{mg}(\text{PO}_4^{3-})/\text{g}$ .

It can be concluded that modified GO and rGO have higher adsorption capacities than those unmodified. Iron oxide decoration was mostly used and the most efficient agent in terms of phosphate capturing rather than Ti and Zr. It might be attributed to its availability, low cost and has better affinity to adsorb phosphate ions rather than Zr and Ti. Table 4 summarises the reported studies of phosphate removal by GO and rGO based adsorbents.

#### 2.4. Carbon nanotubes based adsorbents

Carbon nanotubes (CNTs) are the cylindrical structure of the graphene sheets. CNTs are classified in three main groups according to the number of graphene layers; one rolled layer of graphene known as single-wall (SWCNTs); two rolled layers of graphene known as double wall (DWCNTs); and three or more layers are attributed to what is known as multi-wall (MWCNTs). Due to their high chemical and thermal stabilities, structural properties, large surface area and functionalisation capabilities, the CNTs will be a competitive candidate for the removal of pollutants (Mashkoor and Nasar, 2020). CNTs demonstrate low dispersibility in water and as such, the modification was conducted not only to enhance the adsorption capacity of phosphate, but also to improve their dispersibility in water (Gu et al., 2019). Five reports between 2016 and 2019 were found and reviewed for phosphate removal from aqueous solutions by raw, carboxylated and modified CNTs.

Raw CNTs without modification were first tested for phosphate removal in 2016 by Mahdavi and Akhzari (2016). Raw CNTs with a surface area of 200  $\text{m}^2/\text{g}$  and PZC of 7.1 were found to have a maximum adsorption capacity of 15.4  $\text{mg}(\text{P})/\text{g}$  with a saturation time of 100 min. Their results also indicate that the adsorption process of phosphate by unmodified CNTs is chemical and followed the Freundlich isotherm model. The CNTs were also found to be efficient in removing trace amounts of phosphate from secondary wastewater effluent (Wang et al., 2019). Different studies have reported the modification of CNTs to improve the adsorption capacity of phosphate. The CNTs were either directly modified or carboxylated before modification to enhance their reactivity.

Owing to the positively charged amino groups in chitosan, it has been used for the removal of negatively charged pollutants such as phosphate. Hence, it has been tested to decorate CNTs for phosphate remediation (Huang et al., 2018). In this study, Huang et al. (2018) attached the chitosan to the surface of MWCNTs by simple polymer crosslinking method. The results demonstrated that the maximum adsorption capacity of phosphate was 36.1  $\text{mg}(\text{P})/\text{g}$  and best fitted with the Freundlich isotherm model. The authors concluded that MWCNTs-chitosan adsorbent could be prepared by an extremely simple modification method, demonstrating an exothermic adsorption process with a significantly shorter equilibrium time of 30 min, and following

the pseudo-first order kinetic model with excellent reusability.

Modification of the CNTs with carboxyl groups improves the dispersibility of CNTs in aqueous solutions and increases their reactivity. Carboxylated MWCNTs (MWCNTs-COOH) demonstrated low phosphate adsorption capacity of 2–2.63  $\text{mg}(\text{P})/\text{g}$  (Gu et al., 2019; Zong et al., 2017). However, MWCNTs-COOH, functionalised with different metal such as La and Zr, led to an improvement of the adsorption capacity. For example, Zong et al. (2017) impregnated the surface of commercial MWCNTs-COOH with  $\text{La}(\text{OH})_3$ . The modification and adsorption processes of this study are presented in Fig. 6. La doping has reduced the surface area of MWCNTs-COOH, which was attributed to the blockage of the pores with La. However, the fabricated adsorbent MWCNTs-COOH-La demonstrated an adsorption capacity of 48.02  $\text{mg}(\text{P})/\text{g}$  with an equilibrium time of 110 min. The adsorption mechanism was explained by a ligand exchange mechanism and the formation of inner-sphere complex as confirmed by the intra particle diffusion study. Moreover, Gu et al. (2019), modified the surface of the MWCNTs-COOH by zirconium using the chemical precipitation method. Zirconia has increased the PZC from 5.2 (for MWCNTs-COOH) to 7.2 for (MWCNTs-COOH-Zr), while it reduced the surface area from 500 to 250  $\text{m}^2/\text{g}$ . However, the MWCNTs-COOH-Zr demonstrated an adsorption capacity of 10.9  $\text{mg}(\text{P})/\text{g}$ . Kinetic and isotherm data were best fitted with Elovich and Freundlich models, respectively; suggesting a chemisorption process and the formation of an inner layer complex on the heterogeneous surfaces of the adsorbent, in addition to the electrostatic interactions as illustrated in Fig. S3.

Table 5 presents the applications of CNTs based adsorbents for the removal of phosphate ions. It can be observed that CNTs demonstrated higher capacity than the carboxylated CNTs due to their lower negativity. Modification significantly improved the adsorption capacity, where La has the higher affinity among chitosan and Zr.

#### 2.5. Graphite/graphite oxide based adsorbents

Graphite is a crystalline carbon form in which carbon atoms are organized in a hexagonal structure. The carbon layers in the graphite structure are defined as a graphene sheets, which are connected to one another by the weak van der Waals intermolecular forces. Single layer of carbon sheets is defined as graphene and multi layers are known as graphite (Yuan et al., 2017). There are three types of natural graphite that occur in the environment known as amorphous, flakes and high crystalline graphite. To enhance the reactivity and surface properties, the natural graphite is either oxidised or converted to other forms of graphite such as expanded or exfoliated graphite. Graphite powder, expanded graphite, and graphite oxide have been investigated for the removal of phosphate from aqueous solutions and all of them demonstrate a negligible or a very low adsorption capacity of phosphate (Zhang et al., 2015; Y. Zhang et al., 2016a; Zong et al., 2013). Expanded graphite is an easily preproduced material, low cost, non toxic, low density and high loaded material (Zhang et al., 2015). Graphite oxide has a stable carbon layer structure with a variety of oxygen functional groups such as epoxy, carboxylic, carbonyl and hydroxyl attached to the surfaces and edges of the graphite, which supports various surface modification (Zong et al., 2013). To enhance the phosphate affinity toward the graphite particles; different metal oxides have been doped onto graphite such as La, Mg and zirconia (Zhang et al., 2015; Y. Zhang et al., 2016a; Zong et al., 2013).

Graphite was first tested for phosphate removal in 2013 by Zong et al. (2013) who prepared a graphite oxide from commercial graphite using the Modified Hummers' method. This material was then functionalised with zirconia by the post-grafting technique. The functionalisation of zirconia onto graphite oxide raised the surface area and the PZC of GO from 44.0 to 160.1  $\text{m}^2/\text{g}$  and from negatively charged material over the studied pH range (2–11.3) to a PZC of 2.18, respectively. The adsorption results demonstrated a maximum adsorption capacity of 16.45  $\text{mg}(\text{PO}_4^{3-})/\text{g}$  compared to a negligible removal using the graphite

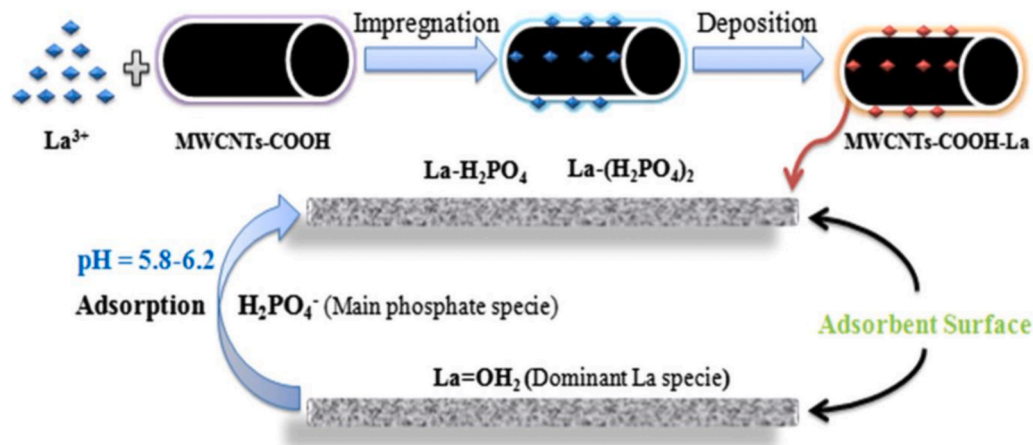


Fig. 6. Schematic presentation of La doping onto MWCNTs-COOH and the adsorption process of phosphate (Zong et al., 2017).

Table 5

Summary of the reported studies of phosphate removal by CNTs based adsorbents.

Adsorbent	Adsorbent synthesis method	Studied phosphate concentration (mg/L)	Surface area ( $\text{m}^2/\text{g}$ )	PZC	$Q_m$ (mg/g)	Kinetics	Isotherm	Adsorbent dose D (g/L), Optimum $\text{pH}_{\text{opt}}$	Adsorption Mechanism	Ref
CNTs	–	25–200 ( $\text{PO}_4^{3-}$ )	200	7.1	15.4 (P) at pH 5, 25 °C	PSO	F	D: 2 $\text{pH}_{\text{opt}}$ : 2 T: 100 min	Chemisorption	Mahdavi and Akhzari (2016)
MWCNTs-chitosan	Polymer crosslinking method for chitosan doping	25–200 (P)	–	–	36.1 (P) at pH 3, 25 °C	PFO, Intra-particle diffusion	F	D: 1 $\text{pH}_{\text{opt}}$ : 3 T: 30 min	Electrostatic interactions	Huang et al. (2018)
MWCNTs-COOH-La	Impregnation for La doping	5–50 (P)	140	–	48.02 (P) at pH 6, 25 °C	PSO, Intra-particle diffusion	L	D: 0.625 $\text{pH}_{\text{opt}}$ : 3 T: 110 min	Ligand exchange, inner sphere complex	Zong et al. (2017)
MWCNTs-COOH-Zr	Chemical precipitation for Zr doping	5–50 (P)	250	7.2	10.9 (P) at pH 6.16, 30 °C	Elovich	F	D: 1 $\text{pH}_{\text{opt}}$ : 3 T: 5 h	Electrostatic interactions, inner layer complex	Gu et al. (2019)

oxide. The adsorption of phosphate onto the modified adsorbent was promoted at low pH as a result of the electrostatic interactions, while the capacity was slightly influenced by increasing the ionic strength and temperature of the solution. Zhang et al. (2015) investigated phosphate

removal from water using expanded graphite impregnated with  $\text{La}_2\text{O}_3$ . The study investigated the effect of the preparation parameters, and it was found that the adsorbed amount of phosphate onto expanded graphite increased reaching a constant value with Lanthanum loading

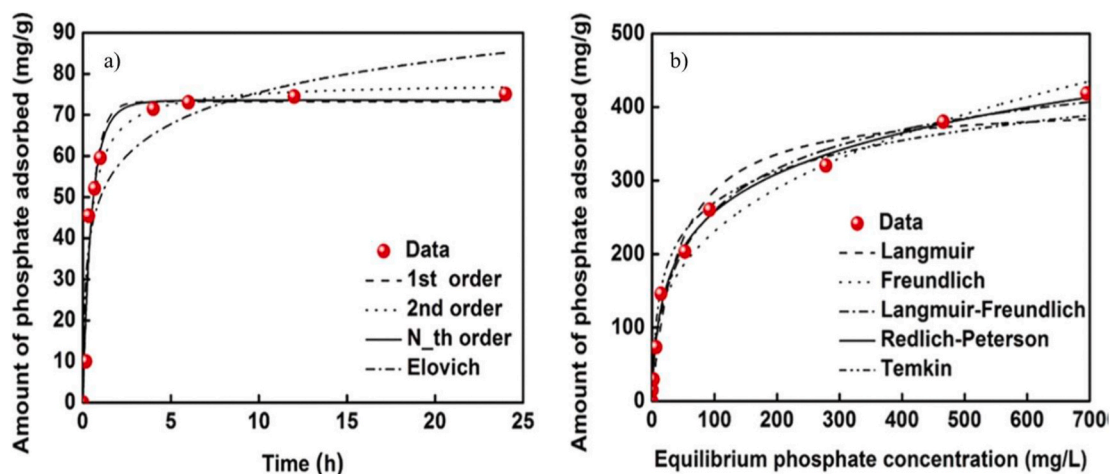


Fig. 7. Adsorption isotherm (a) and kinetics (b) of phosphate removal by MgO-impregnated graphite powder (Y. Zhang et al., 2016b).

and impregnation temperature; while it increased with calcination temperature, whilst there was no effect from impregnation time. Kinetic and equilibrium data were best fitted with the pseudo 2nd order model and the Langmuir isotherm, respectively. The maximum adsorption capacity was 12.6 mg(P)/g and the equilibrium was reached after 480 min of adsorption.

Production of Lithium ion batteries generate significant amounts of graphite powder that it is discharged into the environment. Y. Zhang et al. (2016a, 2016b) enriched this graphite powder with magnesium and tested its ability to capture phosphate from water. The graphite powder was first oxidised with nitric acid and then impregnated with different loadings of MgO. The adsorption results demonstrated a superior adsorption capacity of phosphate onto the engineered adsorbent of 406.3 mg( $\text{PO}_4^{3-}$ )/g at 22 °C, as depicted in Fig. 7. The high adsorption capacity was maintained over a wide range of pH from 1.6 to 10.4. The adsorption kinetics were found to be best fitted with the N-th order model suggesting a multiple mechanism adsorption process. All of the tested isotherms fit the equilibrium data confirming the heterogeneity of the adsorbent surface. This was confirmed by the post sorption characterisations, which concluded that phosphate adsorption onto the fabricated adsorbent is mainly controlled by the precipitation of phosphate to form  $\text{Mg}_3(\text{PO}_4)_2 \cdot 8\text{H}_2\text{O}$  and  $\text{MgHPO}_4 \cdot 1.2\text{H}_2\text{O}$ . The authors concluded that modification of waste materials from the Lithium-ion batteries manufacturing process can provide a novel adsorbent for wastewater treatment to achieve sustainable development.

Table 6 summarises the reported studies of phosphate removal by graphite-based adsorbents. It can be seen that MgO modification demonstrated a superior affinity toward phosphate removal compared to other modifying elements such as La and Zr.

## 2.6. Charcoal based adsorbent

Charcoal is a porous carbon material produced from the incomplete combustion of wood, animal bones, cellulose or plant products. Owing to its low cost and environmentally friendly production process, charcoal has been utilised as an adsorbent for phosphate capture from aqueous solutions. However, similar to other carbon structures, it has a low phosphate adsorption capacity.

Charcoal was tested for phosphate removal in 1982 by Jayson et al. (1982). This study found that the maximum adsorption capacity of  $\text{PO}_4^{3-}$  onto activated charcoal cloths was  $\sim 4.08 \text{ mg}(\text{PO}_4^{3-})/\text{g}$ , in which saturation capacity was reached in 40 min. The prepared charcoal has a surface area, pore volume, average pore diameter, PZC of 1300  $\text{m}^2/\text{g}$ , 0.59  $\text{cm}^3/\text{g}$ , 1.77 nm and 2.7 nm, respectively. The authors explained that phosphate removal by charcoal is a physisorption adsorption controlled by the intraparticle diffusion of phosphate ions into the charcoal pores. In 2013, Khan et al. (2013) investigated the phosphate

removal from water using coal, charcoal, and coal ash adsorbents collected from a local coal mining plant. These adsorbents were vacuum treated at 200 °C to generate inter and intra-particle spacings to accommodate more phosphate molecules. The adsorbents were used in a high dosage of 20 g/L and equilibrium was reached in 45 min. All of the adsorbents demonstrated poor adsorption of phosphate as seen in Fig. 8. However, the vacuumed coal has the highest adsorption capacity of  $\sim 0.114 \text{ mg}(\text{PO}_4^{3-})/\text{g}$  compared to  $\sim 0.024$  and  $\sim 0.021 \text{ mg/g}$  for vacuum treated charcoal and coal ash, respectively. The authors concluded that multi-layer adsorption is occurring, where surface precipitation and surface complex formation are the main mechanisms of adsorption. Mor et al. (2017) determined that the commercial activated charcoal with a surface area of 1000  $\text{m}^2/\text{g}$  has an adsorption capacity of 0.461  $\text{mg}(\text{PO}_4^{3-})/\text{g}$  where the equilibrium was reached in 2 h. The study declared that adsorption of phosphate onto activated charcoal is a chemisorption process, where the kinetics and isotherms follow the pseudo second order and Langmuir models, respectively.

A better performing adsorption capacity was obtained by Yuan et al. (2014) who reported phosphate removal by commercial barbecue bamboo charcoal (BBC). The BBC has a carbon content of 86.4% with a surface area, pore volume and average pore radius of 273.38  $\text{m}^2/\text{g}$ , 0.12  $\text{cm}^3/\text{g}$ , and 1.77 nm, respectively. The equilibrium time was reached in 2 h with a maximum Langmuir adsorption capacity of 1.07  $\text{mg}(\text{P})/\text{g}$ . The authors provided the optimised conditions for the removal of phosphate using BBC and these were as follows, average particle size 0.15–0.18

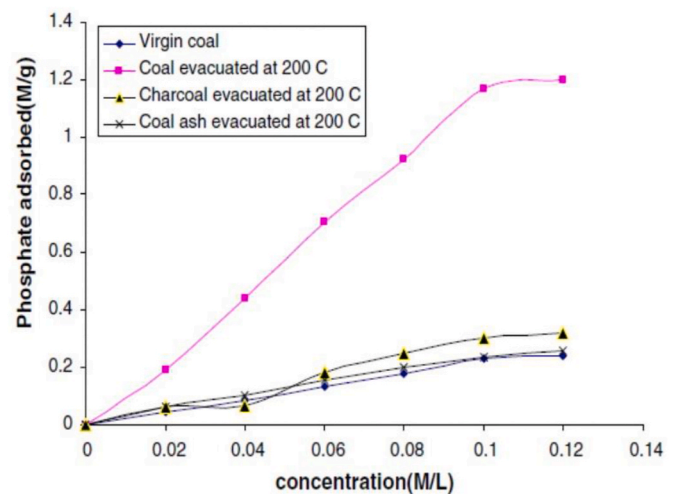


Fig. 8. Phosphate adsorption onto coal, charcoal, and coal ash (Khan et al., 2013).

Table 6

Summary of the reported studies of phosphate removal by graphite-based adsorbents.

Adsorbent	Adsorbent synthesis method	Studied phosphate concentration (mg/L)	Surface area ( $\text{m}^2/\text{g}$ )	PZC	$Q_m$ (mg/g)	Kinetics	Isotherm	Adsorbent dose D (g/L), Optimum pH, Equilibrium time (T)	Adsorption mechanism	Ref
Expanded graphite loaded with LaO	Impregnation method.	10–80 (P)	–	8.1	12.6 (P) at 25 °C	PSO	L	D: 2 pH <sub>opt</sub> : 4 T: 480 min	Electrostatic interactions Ion exchange Lewis	Zhang et al. (2015)
Graphite oxide loaded with Zr	Modified Hummers method to produce GO and post-grafting method for functionalisation.	10–50 ( $\text{PO}_4^{3-}$ )	160.1	2.18	16.45 ( $\text{PO}_4^{3-}$ ) at pH 6, 25 °C	PSO	L	D: 0.5 pH <sub>opt</sub> : 2 T: 1200 min for $C_0$ 20 ppm	acid–base interaction	Zong et al. (2013)
Graphite powder enriched with Mg	Graphite powder was oxidised by nitric acid followed by Mg Impregnation.	30.6–1532.3 ( $\text{PO}_4^{3-}$ )	33.54	–	406.3 ( $\text{PO}_4^{3-}$ ) at 22 °C	N <sup>th</sup> order model	L, F, L-F, Timken, Redlich–Peterson	D: 2 pH <sub>opt</sub> : 1.6–8.6 T: 4 h	Precipitation	(Y. Zhang et al., 2016a; 2016b)



mm, adsorbent dose 10 g/L, pH 5 and temperature of 30 °C. The authors also found that phosphate adsorption onto BBC is a chemisorption process.

The applications of charcoal materials for the removal of phosphate ions are presented in Table S5. Charcoal adsorbents demonstrated low adsorption capacities of phosphate. However, their high surface area suggests that the modification of these materials and testing for different pollutants removal may yield more promising results.

## 2.7. Other carbon materials

This section summarises the reported studies of phosphate removal by carbon nanofibers, carbon fibre paper, mesoporous carbon CMK-3, fabricated porous carbon and carbide derived carbon.

X. Zhang et al. (2016) used Lanthanum carbon nanofibers (LaCNFs) prepared by the carbonisation of electrospun polyacrylonitrile nanofibers containing La-species. The CNFs loaded by lanthanum have a PZC of 9.8 and shows higher surface area than the free lanthanum CNFs (41.8 m<sup>2</sup>/g for LaCNFs and 27.1 m<sup>2</sup>/g for CNFs). LaCNFs illustrates a phosphate adsorption capacity of 20.51 mg(P)/g in which the equilibrium time was ~250 min. Carbon fibre papers doped by MgO were investigated by Ahmed et al. (2018). The adsorption results indicated that CF/MgO-400 can adsorb phosphate 9 times more than the CF. Hu et al. (2018) utilised the Sisal biomass for carbon fibre production. In this study, the carbon fibres were modified by Cu–Al LDH and illustrated a maximum phosphate adsorption capacity of 105.26 mg(P)/g at 15 °C.

CMK-3 is a mesoporous carbon material prepared from the hexagonal SBA-1. CMK-3 was used as a substrate to load zirconium oxide or amino groups to improve the removal of phosphate from aqueous solutions (Ju et al., 2016; Yang et al., 2018). For example, Ju et al. (2016) investigated phosphate removal from water by mesoporous carbon CMK-3 decorated by zirconium oxide (ZrO<sub>2</sub>@CMK-3). The study found that the optimised ZrO<sub>2</sub> loading onto the CMK-3 is 29.5 wt%. The adsorption capacity was increased from ~2 mg(P)/g for CMK-3 to ~20 mg(P)/g for 29.5%ZrO<sub>2</sub>@CMK-3. Yang et al. (2018) functionalised the CMK-3 with aminopropyl (APTMS-CMK-3) by the post grafting method. The PZC increased from 3.9 to 7.3, thus confirming the successful functionalisation of aminopropyl. APTMS-CMK-3 has a higher adsorption capacity of about 40 mg(P)/g compared to 1.99 mg(P)/g for CMK-3. In comparison with ZrO<sub>2</sub>@CMK-3, APTMS-CMK-3 demonstrated faster kinetics and a higher adsorption capacity under similar conditions, most probably attributed to the higher PZC of APTMS@CMK-3.

Porous carbon obtained from the thermal treatment of sucrose and lignin have been loaded with lanthanum and demonstrated a significant enhancement in the adsorption capacity of phosphate (Koilaraj and Sasaki, 2017; Liu et al., 2019). Recently, Almanassra et al. (2020b) investigated the removal of phosphate by carbide derived carbon (CDC), which is a new carbon material that has tunable properties and could be prepared from different carbides Almanassra et al. (2020c). Structural characterisation of CDC indicates a closer form of a graphitic material, where the CDC demonstrated a surface area of 1120 m<sup>2</sup>/g with an adsorption capacity higher than 16 mg(PO<sub>4</sub><sup>3-</sup>)/g, which was attributed to its high PZC. The EDS/SEM analysis illustrates an even distribution of phosphate ions onto the surface of CDC as demonstrated in Fig. S4. Table S6 provides the application of different carbon structures for the removal of phosphate.

## 3. Adsorption mechanisms

The adsorption mechanism is of significant importance to understand the interaction between phosphate ions and the adsorbent molecules. The mechanism of adsorption is also the core element of controlling the adsorption kinetics, energy, capacity and thermodynamics. For the reader's convenience, the authors have summarised the adsorption mechanisms of the reviewed papers in Table 2–6, S1 – S6. The chemical or physical adsorption of phosphate onto modified and

unmodified carbonaceous adsorbents was explained by different mechanisms, such as, electrostatic interactions, ion exchange, ligand exchange, precipitation, Lewis acid–base interaction, inner sphere complexation and outer sphere complexation. The adsorption mechanism is highly dependent on the nature, charge and molecular content of the adsorbent. The adsorption mechanism also varies with pH and different adsorption mechanisms can be found in the same adsorption system. For instance, the adsorption of phosphate onto La-modified graphene involves the formation of inner and outer sphere complexes, chemical bonding and electrostatic interactions as seen in Fig. 9.

Most carbon-based adsorbents involve phosphate adsorption by electrostatic interactions. This is because phosphate ions are negatively charged and carbon adsorbents generally demonstrate a particle surface charge. The electrostatic interaction mechanism might occur due to physical and chemical adsorption. The pH of the solution significantly affects the electrostatic adsorption process. This is attributed to the fact that phosphate protonation is changeable with pH, and the carbon adsorbent surface also changes with pH. In general, the electrostatic interactions occur when the pH of the solution is lower than the PZC of the adsorbent, whereby the negatively charged phosphate ions are electrostatically attracted to the positively charged carbon adsorbent. Once the pH of the solution exceeds the PZC, no more electrostatic adsorption takes place. However, if adsorption is occurring at pH>PZC, this implies that other adsorption mechanisms are taking place. The electrostatic interaction adsorption is considered to be reversible in which desorption of phosphate occurs easily (Loganathan et al., 2014).

The ion exchange mechanism of phosphate adsorption onto the carbon-based adsorbents is related to ion replacement, implying that an attached ion on the adsorbent surface leaves the structure of the adsorbent and is substituted by similar ion numbers of phosphate ions, such as the phosphate exchange with chloride ions. The ion exchange mechanism is considered as weak adsorption, reversible and expressed in material characterisation by the formation of outer sphere complexes (Loganathan et al., 2014). This phenomenon also occurs in both physical and chemical adsorption processes. The ligand exchange mechanism is similar to the ion exchange mechanism of replacing the ions, however, in this mechanism the replacement is occurring between the phosphate ions and the (OH) groups onto the surface of the adsorbent. An example of the phosphate sorption by ligand exchange is the iron modified-GAC (Braun et al., 2019; Kumar et al., 2017). The ligand exchange mechanism is related to the chemical adsorption processes, with stronger adsorption than an ion exchange mechanism and hardly reversible. The ligand exchange mechanism is expressed in material characterisation by the formation of inner sphere complexes.

The adsorption of phosphate on metal modified carbon adsorbents might occur by surface precipitation. In fact, the precipitation of a component will occur if its concentration exceeds its solubility product in the solution. The precipitation of phosphate as metals phosphates was observed in materials characterization for most of the Mg modified graphite and AC (Y. Zhang et al., 2016a, 2016b; Zhu et al., 2018), moreover, metal phosphates were detected for Ca and Zn modified AC and GAC (Bhargava and Sheldarkar, 1993; Kilpimaa et al., 2014; Ouakouak et al., 2017). The surface precipitation mechanism is considered as a fast adsorption process and not easily reversible.

The Lewis acid-base interaction was also a controlling mechanism for phosphate adsorption onto carbon-based adsorbents. Under acidic conditions, the concentration of H<sup>+</sup> ions is high, which protonates the modified element on the adsorbent, thus, becoming a weak acid and working as an electron acceptor. The phosphate ions in acidic media are considered as weak bases and function as electron donors. This phenomenon is reversed in the alkaline conditions. Accordingly, the electron donor-acceptor interaction is occurring between phosphate ions and the elements attached onto the carbon adsorbents. Examples of phosphate sorption by Lewis acid base interactions are La modified ACF (Liu et al., 2013, 2011; L. Zhang et al. 2016a,b,c,d; Zhang et al., 2012b, 2012a, 2011).

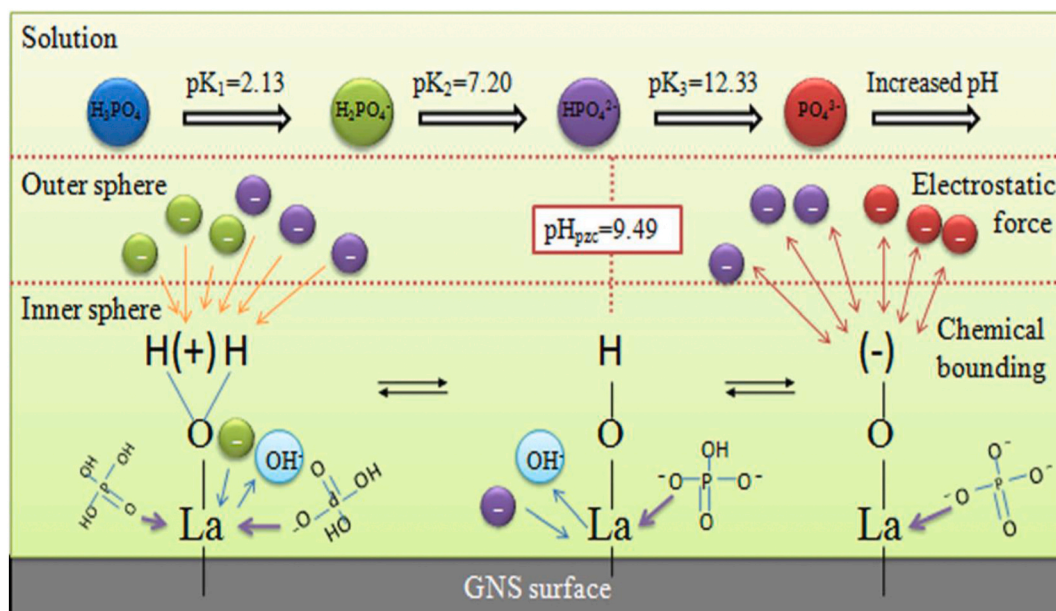


Fig. 9. Adsorption mechanisms of phosphate onto La modified graphene nanosheets (Zhang et al., 2014).

Other mechanisms such as  $\pi$ - $\pi$  interactions were found to be less favourable to control the adsorption of phosphate onto modified graphene adsorbents. It was detected to control the adsorption of phosphate onto La modified magnetic graphene (Nodeh et al., 2017). The diffusion of adsorbate molecules within the adsorbent pores always remains one of the mechanisms of phosphate molecules adsorption onto carbonaceous adsorbents. However, it is considered an extremely slow process and related to the physical mechanism adsorption processes.

#### 4. Adsorption thermodynamics

The thermodynamic parameters provide essential information about the adsorption of phosphate ions onto the adsorbent surface. Measuring the values of Gibbs free energy ( $\Delta G^\circ$ ), enthalpy ( $\Delta H^\circ$ ) and entropy ( $\Delta S^\circ$ ) of adsorption can be utilised to imply the spontaneity and nature of the adsorption process. The negative and positive values of ( $\Delta H^\circ$ ) indicate that the adsorption is exothermic and endothermic process, respectively. The negative value of ( $\Delta G^\circ$ ) indicates a spontaneous adsorption process, while the positive value of ( $\Delta S^\circ$ ) is related to the increase in the degree of the randomness at the liquid/solid interface.

All of the reviewed studies investigated the thermodynamic parameters of adsorption reported a negative  $\Delta G^\circ$  values of phosphate adsorption onto modified and unmodified carbon-based adsorbents indicating that phosphate removal by such adsorbents is spontaneous in nature. Based on the estimated enthalpy values, the adsorption of phosphate was found to be an endothermic adsorption process as suggested by the positive value of  $\Delta H^\circ$  with some exceptional cases that found an exothermic adsorption process, such as phosphate removal by chitosan modified MWCNT (Huang et al., 2018) and activated carbon cloths (Jayson et al., 1982). The  $\Delta S^\circ$  values were found to be positive for the majority of the studies indicating the strong affinity of phosphate ions towards these adsorbents and its randomness increase at the solid solution interface. The only exception was found for the activated charcoal, where a decrease in the randomness was obtained as demonstrated by a negative value of  $\Delta S^\circ$  (Mor et al., 2017).

#### 5. Effect of competing ions

In actual wastewater, municipal and industrial water, phosphate ions exist with other ions that might compete with phosphate for the active adsorption sites. Therefore, it is important to investigate the effect of

coexisting ions onto the adsorption of phosphate. Investigating such factors can provide an important information about the practical applications of the adsorbents. In general, phosphate exists with a variety of inorganic anions such as  $\text{SO}_4^{2-}$ ,  $\text{CO}_3^{2-}$ ,  $\text{HCO}_3^-$ ,  $\text{NO}_3^-$ ,  $\text{Cl}^-$  and  $\text{F}^-$ . Other pollutants, such as, humic acids and pharmaceuticals could also be found in the water effluents.

The existence of inorganic anions have been found to influence the adsorption capacity of phosphate onto carbonaceous adsorbents (Chen et al., 2016; Gu et al., 2019). Amongst the investigated coexisted anions, it can be concluded that; the divalent anions  $\text{SO}_4^{2-}$  and  $\text{CO}_3^{2-}$  which have a higher charge density can be removed faster than the univalent anions  $\text{Cl}^-$  and  $\text{NO}_3^-$ , and consequently they have higher impact on the phosphate adsorption capacity (Luo et al., 2016). The presence of  $\text{CO}_3^{2-}$  ions was found to have the largest effect among these four anions (Zhang et al., 2012a, 2015; Zong et al., 2017). This was attributed to several reasons: i)  $\text{CO}_3^{2-}$  has a strong affinity toward the active adsorption sites; ii) the addition of  $\text{CO}_3^{2-}$  increases the pH of the solution, which decreases the phosphate removal; and iii) for the case of La modified carbon adsorbents, the negative effect of  $\text{CO}_3^{2-}$  was attributed to the smaller Ksp value of  $\text{La}_2(\text{CO}_3)_3$  ( $3.98 \times 10^{-34}$ ) compared to  $\text{LaPO}_4$  ( $3.7 \times 10^{-23}$ ), which implies the formation of  $\text{La}_2(\text{CO}_3)_3$ . The  $\text{HCO}_3^-$  ion was found to have a lower effect than carbonate ions, however, its obvious reduction may also be attributed to the rise in pH that is not favourable for phosphate adsorption (Zong et al., 2017). The  $\text{SO}_4^{2-}$  ions has an obvious effect on the removal of phosphate as demonstrated in several studies (Huong et al., 2019; Karthikeyan and Meenakshi, 2019; Khalil et al., 2017; Namasivayam and Sangeetha, 2004). The effect of sulphate was attributed to its ionic radius (0.230 nm), which is close to phosphate ions radius (0.238), and encourages the sulphate to compete for the same adsorption sites of phosphate (Almanassra et al., 2020b). In comparison,  $\text{NO}_3^-$  and  $\text{Cl}^-$  were found to have lower impact on the adsorption capacity of phosphate on carbon based adsorbents, even when their concentration is 15 times higher than phosphate (Huong et al., 2019; Namasivayam and Sangeetha, 2004). The  $\text{F}^-$  ions were found to have a negative impact on the removal of phosphate, which was attributed to its strong electronegativity encouraging it's linkage with the protonated adsorbent surface and hence decreased the adsorption capacity of phosphate (Liu et al., 2013; Xiong et al., 2017; Zhang et al., 2014; Zhou et al., 2012).

Several experimental studies have reported the effect of natural organic matter on phosphate removal. The coexistence of humic acid

with phosphate was found to reduce the adsorption capacity of phosphate and its effect was more significant with its increasing concentration (Khalil et al., 2017; Koilraj and Sasaki, 2017; Mahdavi and Akhzari, 2016). Organic matters possess an affinity towards the active adsorption sites and then competes with phosphate therefore decreasing the phosphate adsorption capacity.

## 6. Desorption studies

Good performing adsorbents for phosphate removal should demonstrate high adsorption capacity, cost effectiveness and the ability to be regenerated/reused for a long period. Adsorbent regeneration remains challenging and the expensive part of the adsorption process. Desorption of phosphate from modified and unmodified carbon-based adsorbents has been carried out using salt, acids and alkaline solutions. Salts such as NaCl were found to be efficient for phosphate desorption from the adsorbents that have weak binding between phosphate and the adsorbent surface, in which the adsorption mechanism is controlled by outer sphere complexes (Xu et al., 2015). However, salts were found ineffective for phosphate desorption where chemical reactions are involved and where strong binding between phosphate and the adsorbent surface exists (Zhang et al., 2012a, 2012b). Acids and alkaline solutions were found to be efficient for phosphate desorption in such cases. The use of acids and alkaline solutions with  $\text{pH} < 3$  or higher  $> 10$  are feasible, however, these ranges are unfavourable for phosphate adsorption anyway. The phosphate is uncharged at  $\text{pH} < 3$  and therefore, it is not easily adsorbed, while phosphate has negative charge at  $\text{pH} > 10$  where the repulsion forces increase with the adsorbent surface, and hence result in low adsorption removal. Moreover,  $\text{OH}^-$  ions compete with phosphate ions on the active adsorption sites at  $\text{pH} > 10$  and therefore results in low phosphate removal.

Different acids and alkaline solutions were used for desorption of phosphate from carbon based adsorbents such as NaOH (Gu et al., 2019; Harijan and Chandra, 2017; Namasivayam and Sangeetha, 2004), HCl (Namasivayam and Sangeetha, 2004), ethanol (Gu et al., 2019), acetone and  $\text{HNO}_3$  (Kumar et al., 2010). It was observed from these desorption efficiencies that the desorption efficiencies of alkaline solutions were higher than the desorption efficiencies of acid solutions (Gu et al., 2019; Harijan and Chandra, 2017). This might be attributed to the fact that most of the studies have reported higher phosphate removal at low pH compared to high pH, which makes alkaline solutions more suitable for phosphate desorption from carbonaceous adsorbents. The NaOH solutions were found to be the most commonly used for desorption of phosphate (Gu et al., 2019; Harijan and Chandra, 2017; Karthikeyan and Meenakshi, 2019; Khalil et al., 2017; Zhang et al., 2012a). Most exhausted adsorbents washed by NaOH solutions demonstrated a desorption efficiency over 70% of their initial adsorption capacity for 3–5 cycles (Huang et al., 2018; Nodeh et al., 2017; Zong et al., 2013). For example, Huang et al. (2018) found that the adsorption capacity of phosphate onto chitosan modified MWCNT could be maintained more than 94% even after 5 adsorption/desorption cycles by regeneration using 0.1 mol/L NaOH. However, due to strong chemical binding between phosphate and some adsorbents such as  $\text{ZnCl}_2$  modified AC (Namasivayam and Sangeetha, 2004), the phosphate ions were not easily desorbed by NaOH. Increasing the concentration of NaOH was found to increase the desorption efficiency, for instance, Xiong et al. (2017), found that the desorption efficiency increased from 5.18 to 91.4% by increasing the NaOH concentration from 0.001 to 0.1 mol/L. However, further increasing the NaOH concentration has no significant enhancement on the desorption efficiency. It should be noted that the desorption efficiency decreased with regeneration cycles due to the loss of functional groups onto the adsorbent surface (Bai et al., 2018; Sakamoto et al., 2020).

## 7. Knowledge gaps and research recommendations

Phosphate removal by carbonaceous materials is a growing area and the number of annual publications in this field is increasing. However, there are several challenging questions that require further investigation. As such, the research needs and critical issues are summarised below:

- It should be noted that thus far all of the reported investigations on phosphate removal by carbon-based materials have been carried out on lab scale experiments. The economic feasibility and cost-effective analysis should be considered for pilot and larger scale up processes.
- Very few studies have implemented the continuous flow experiments. Most of the research of phosphate removal by carbon-based adsorbents concentrated on batch adsorption experiments. Continuous experiments are required to have a robust adsorbent investigation and could provide a better understanding of the actual applications. In this regard, the continuous flow experiments are needed to be explained for phosphate in aqueous solutions, actual waters and complex mixtures.
- Very few studies have investigated the effectiveness of the adsorbent for phosphate removal at high and low concentrations levels. The adsorbent performance is not only evaluated by the maximum adsorption capacity, it should also be effective in adsorbing phosphate at low concentrations. As such, it is recommended to conduct the adsorption experiments at low and high phosphate concentration levels.
- Most of the adsorption equilibrium capacity research papers only apply one or two isotherm models because there are a number of potential adsorption mechanisms involved. As such, more isotherm models are needed to be applied in order to obtain the best capacity predictive model for designing the treatment plant.
- A key factor in the design and sizing of the phosphate adsorption plant is the rate and hence the kinetics of the adsorption step, where the faster the kinetics the smaller (and hence the capital cost) the treatment plant requirement to treat a fixed volume of wastewater.
- It was observed that co-existing ions with phosphate affect the adsorption of phosphate by carbon-based adsorbents. It should also be noted that there is a lack of data on phosphate removal from complex mixtures or multi component system.
- Modification of carbon materials has been found to significantly improve the adsorption capacity of phosphate. However, carbon modification methods consume chemicals and pose environmental issues due to metal leakage. As such, there is always a need for novel eco-friendly techniques for carbon materials modification.
- Separation of the exhausted adsorbent is an issue, where membrane filtration and centrifugation were suggested techniques to separate the used adsorbent. However, centrifugation requires energy and filtration consumes material and suffers from the blockage of pores. Even magnetic adsorbents were successfully employed for the adsorbent separation, and efforts are still required in this area.
- For future investigations, more focus should be given to the adsorbent regeneration, desorption and recovery of both adsorbent and phosphate. This is directly linked with the economic feasibility of the adsorption process. In the literature, the regeneration experiment was performed for only a few studies along with a few number of regeneration cycles. As such, future studies should focus on adsorbents that can be easily regenerated for several adsorption/desorption cycles.
- Phosphate recovery from carbonaceous adsorbents is still at the experimental stage of research, which should be expanded in the future.
- Future studies should consider Life Cycle Assessment studies covering all stages of the adsorption process, from preparation to regeneration, the final destination of the adsorbents and the final destination of the water used. For these studies, it would also be



relevant to have complete studies that include the percentages of recovery obtained in various cycles of use of the adsorbent.

## 8. Conclusions

The review presented analyses and summarises the literature of phosphate removal from aqueous solutions by modified and unmodified carbon based materials such as AC, CNTs, graphite, graphene, graphene oxide and charcoal using the adsorption process. The adsorbent preparation methods, adsorption behaviour, experimental conditions, isotherms, kinetics, and mechanisms of phosphate removal by the different carbonaceous materials were reported. Moreover, the effect of competing ions, adsorption thermodynamics and desorption studies of phosphate have been also outlined.

In general, the adsorption of phosphate by carbon materials is affected by the surface chemistry of the adsorbent such as surface charge, pore characteristics, functional groups, modification element and surface area. Moreover, it is also affected by the experimental conditions such as temperature, pH and the coexisting ions. Regardless of the type of the carbon material, the modified carbonaceous adsorbents demonstrated a significantly higher phosphate adsorption capacity than the un-modified adsorbents. This was mainly attributed to the negative charge existing in nature on most of the raw carbonaceous adsorbents, which is considered unfavourable for the adsorption of negatively charged phosphate ions.

Different metal oxides and hydroxides such as Fe, Mg, Zn and La were used for carbon adsorbents modification. However, due to the variation in the experimental set-up and the sources of the feedstock, it was difficult to claim the best modifying element for phosphate removal, although Mg modification demonstrated the best affinity toward adsorbing phosphate ions. This was attributed to: (i) high PZC of Mg nanoparticles which is around 12, which facilitates the electrostatic interactions over a wide range of pH and hence higher phosphate removal, and (ii) adsorption of phosphate onto Mg modified carbonaceous adsorbents involve several adsorption mechanisms such as precipitation, ligand exchange and electrostatic interactions in the same adsorption process. Iron has been widely used for carbonaceous adsorbents modification, it contributed toward improving the adsorption capacity of phosphate, and moreover magnetic modified adsorbents provide an advantage for the magnetic separation of the adsorbents after use.

Thermodynamic analysis of phosphate removal by carbon-based adsorbents was frequently an endothermic adsorption process and spontaneous in nature. Phosphate in actual municipal water coexists with different ions, where it was found that carbonate anions has the biggest negative effect on the adsorptive removal of phosphate. The optimum pH of phosphate removal was found to be in the range between 3 and 10 for most studies, whilst highly acidic and highly alkaline conditions were found unfavourable for phosphate removal. Desorption of phosphate by NaOH solutions was found the most effective desorption solution. However, it was not efficient for the adsorbents that forms strong binding with phosphate. Despite the progress of phosphate removal by the different carbonaceous adsorbents, several research gaps and future recommendation have been identified and outlined.

## Declaration of competing interest

The authors declare that they have no known competing financial interests or personal relationships that could have appeared to influence the work reported in this paper.

## Acknowledgements

The authors would like to acknowledge Hamad Bin Khalifa University (HBKU, Qatar Foundation, Qatar). The open access funding provided by Qatar National Library.

## Appendix A. Supplementary data

Supplementary data to this article can be found online at <https://doi.org/10.1016/j.jenvman.2021.112245>.

## References

- Ahmed, S., Ashiq, M.N., Li, D., Tang, P., Feng, Y., 2018. Carbon fiber paper @ MgO films : in situ fabrication and high-performance removal capacity for phosphate anions. *Environ. Sci. Pollut. Res.* 25, 34788–34792.
- Ahmed, S., Ashiq, M.N., Li, D., Tang, P., Leroux, F., Feng, Y., 2019. Recent progress on adsorption materials for phosphate removal. *Recent Pat. Nanotechnol.* 13, 3–16.
- Akram, M., Ahmed, S., Li, L., Akhtar, N., Ali, S., 2019. Engineering N-doped reduced graphene oxide decorated with Fe<sub>3</sub>O<sub>4</sub> composite: stable and magnetically separable adsorbent solution for high performance phosphate removal. *J. Environ. Chem. Eng.* 7, 103137.
- Al-zboon, K.K., 2018. Phosphate removal by activated carbon–silica nanoparticles composite, kaolin, and olive cake. *Environ. Dev. Sustain.* 20, 2707–2724.
- Almanassra, I.W., Kochkodan, V., Ponnusamy, G., Mckay, G., Atieh, M., Al-ansari, T., 2020a. Carbide Derived Carbon (CDC) as novel adsorbent for ibuprofen removal from synthetic water and treated sewage effluent. *J. Environ. Health Sci. Engineer* 18, 1375–1390, 2020.
- Almanassra, I.W., Mckay, G., Kochkodan, V., Atieh, M., Al-ansari, T., 2021. A state of the art review on phosphate removal from water by biochars. *Chem. Eng. J.* 409, 128211.
- Almanassra, I.W., Kochkodan, V., Subeh, M., Mckay, G., Atieh, M., Al-ansari, T., 2020b. Phosphate removal from synthetic and treated sewage effluent by carbide derived carbon. *J. Water Process Eng.* 36, 101323.
- Almanassra, I.W., Okonkwo, E.C., Alhassan, O., Atieh, M.A., Kochkodan, V., Al-ansari, T., 2020c. Stability and thermophysical properties test of carbide-derived carbon thermal fluid; a comparison between functionalised and emulsified suspensions. *Powder Technol.* 377, 415–428.
- Bacelo, H., Pintor, A.M.A., Santos, S.C.R., Boaventura, R.A.R., Botelho, C.M.S., 2020. Performance and prospects of different adsorbents for phosphorus uptake and recovery from water. *Chem. Eng. J.* 381, 122566.
- Bai, L., Yuan, L., Ji, Y., Yan, H., 2018. Effective removal of phosphate from aqueous by graphene oxide decorated with  $\alpha$ -Fe<sub>2</sub>O<sub>3</sub> : kinetic, isotherm, thermodynamic and mechanism study. *Arabian J. Sci. Eng.* 43, 3611–3620.
- Bhargava, D.S., Sheldarkar, S.B., 1993. Use of TNSAC in phosphate adsorption studies and relationships. *Isotherm relationships and utility in the field. Water Res.* 27, 325–335.
- Braun, J.C.A., Borba, C.E., Godinho, M., Perondi, D., Schontag, J.M., Wenzel, B.M., 2019. Phosphorus adsorption in Fe-loaded activated carbon : two-site monolayer equilibrium model and phenomenological kinetic description. *Chem. Eng. J.* 361, 751–763.
- Chen, M., Huo, C., Li, Y., Wang, J., 2016. Selective adsorption and efficient removal of phosphate from aqueous medium with Graphene–Lanthanum composite. *ACS Sustain. Chem. Eng.* 4, 1296–1302.
- Dai, H., Han, T., Sun, T., Zhu, H., Wang, X., Lu, X., 2021. Nitrous oxide emission during denitrifying phosphorus removal process: a review on the mechanisms and influencing factors. *J. Environ. Manag.* 278, 111561.
- Dikin, D.A., Stankovich, S., Zimney, E.J., Piner, R.D., Dommett, G.H.B., Evmenenko, G., Nguyen, S.T., Ruoff, R.S., 2007. Preparation and characterization of graphene oxide paper. *Nature* 448, 457–460.
- Ferro, G., Carrasco, M., Rivera, U., Utrera, H., Moreno, C., 1990. The use of activated carbon columns for the removal of ortho-phosphate ions from aqueous solutions. *Carbon N. Y.* 28, 91–95.
- Ghorbani, M., Seyedin, O., Aghamohammadhassan, M., 2020. Adsorptive removal of lead (II) ion from water and wastewater media using carbon-based nanomaterials as unique sorbents : a review. *J. Environ. Manag.* 254, 109814.
- Gu, Y., Yang, M., Wang, W., Han, R., 2019. Phosphate adsorption from solution by zirconium-loaded carbon nanotubes in batch mode. *J. Chem. Eng. Data* 64, 2849–2858.
- Haley, S.T., Alexander, H., Juhl, A.R., Dyhrman, S.T., 2017. Transcriptional response of the harmful raphidophyte *Heterosigma akashiwo* to nitrate and phosphate stress. *Harmful Algae* 38, 258–270.
- Han, T., Lu, X., Sun, Y., Jiang, Jianchun, Yang, W., Pär, G.J., 2020. Magnetic bio-activated carbon production from lignin via a streamlined process and its use in phosphate removal from aqueous solutions. *Sci. Total Environ.* 708, 135069.
- Harijan, D.K.L., Chandra, V., 2017. Akaganeite nanorods decorated graphene oxide sheets for removal and recovery of aqueous phosphate. *J. Water Process Eng.* 19, 120–125.
- Hu, F., Wang, M., Peng, X., Qiu, F., Zhang, T., Dai, H., Liu, Z., Cao, Z., 2018. High-efficient adsorption of phosphates from water by hierarchical CuAl/biomass Carbon fiber layered double hydroxide. *Colloids Surfaces A Physicochem. Eng. Asp.* 555, 314–323.
- Huang, W., Zhang, Y., Li, D., 2017. Adsorptive removal of phosphate from water using mesoporous materials : a review. *J. Environ. Manag.* 193, 470–482.
- Huang, Y., Lee, X., Macazo, F.C., 2018. A sustainable adsorbent for phosphate removal: modifying multi-walled carbon nanotubes with chitosan. *J. Mater. Sci.* 53, 12641–12649.
- Huong, P.T., Jitae, K., Giang, B.L., Nguyen, T.D., Thang, P.Q., 2019. Novel lanthanum-modified activated carbon derived from pine cone biomass as ecofriendly bio-



- sorbent for removal of phosphate and nitrate in wastewater. *Rendiconti Lincei. Sci. Fis. Nat.* 30, 637–647.
- Ibrahim, W., Nodeh, H.R., Sanagi, M.M., 2016. Graphene-based materials as solid phase extraction sorbent for trace metal ions, organic compounds and biological sample preparation. *Crit. Rev. Anal. Chem.* 46, 267–283.
- Irwin, N.B., Irwin, E.G., Martin, J.F., Aracena, P., 2018. Constructed wetlands for water quality improvements: benefit transfer analysis from Ohio. *J. Environ. Manag.* 206, 1063–1071.
- Jayson, G.G., Lawless, T.A., Fairhurst, D., 1982. The adsorption of organic and inorganic phosphates onto a new activated carbon adsorbent. *J. Colloid Interface Sci.* 86, 397–410.
- Ju, X., Hou, J., Tang, Y., Sun, Y., Zheng, S., Xu, Z., 2016. ZrO<sub>2</sub> nanoparticles confined in CMK-3 as highly effective sorbent for phosphate adsorption. *Microporous Mesoporous Mater.* 230, 188–195.
- Karthikeyan, P., Meenakshi, S., 2019. Synthesis and characterization of Zn–Al LDHs/activated carbon composite and its adsorption properties for phosphate and nitrate ions in aqueous medium. *J. Mol. Liq.* 296, 111766.
- Khalil, A.M.E., Eljamal, O., Amen, T.W.M., Sugihara, Y., Matsunaga, N., 2017. Optimised nano-scale zero-valent iron supported on treated activated carbon for enhanced nitrate and phosphate removal from water. *Chem. Eng. J.* 309, 349–365.
- Khan, S., Ishaq, M., Ahmad, I., 2013. Evaluation of coal as adsorbent for phosphate removal. *Arab. J. Geosci.* 6, 1113–1117.
- Kilpimaa, S., Runtti, H., Kangas, T., Lassi, U., Kuokkanen, T., 2015. Physical activation of carbon residue from biomass gasification: novel sorbent for the removal of phosphates and nitrates from aqueous solution. *J. Ind. Eng. Chem.* 21, 1354–1364.
- Kilpimaa, S., Runtti, H., Kangas, T., Ulla, L., Kuokkanen, T., 2014. Removal of phosphate and nitrate over a modified carbon residue from biomass gasification. *Chem. Eng. Res. Des.* 92, 1923–1933.
- Koilraj, P., Sasaki, K., 2017. Selective removal of phosphate using La-porous carbon composites from aqueous solutions: batch and column studies. *Chem. Eng. J.* 317, 1059–1068.
- Kumar, P., Sudha, S., Chand, S., Srivastava, V.C., Kumar, P., Sudha, S., Chand, S., Srivastava, V.C., 2010. Phosphate removal from aqueous solution using coir-pith activated carbon phosphate removal from aqueous solution using coir-pith activated carbon. *Separ. Sci. Technol.* 45, 1463–1470.
- Kumar, S., Prot, T., Korving, L., Keesman, K.J., Dugulan, I., Loosdrecht, M.C.M., Van, Witkamp, G., 2017. Effect of pore size distribution on iron oxide coated granular activated carbons for phosphate adsorption—Importance of mesopores. *Chem. Eng. J.* 326, 231–239.
- Kumwimba, M., Dzakpasu, M., Li, X., 2020. Potential of invasive watermilfoil (*Myriophyllum* spp.) to remediate eutrophic waterbodies with organic and inorganic pollutants. *J. Environ. Manag.* 270, 110919.
- Kyong, W., Kyong, Y., Sung, H., Tae, J., 2014. Optimization of coagulation/flocculation for phosphorus removal from activated sludge effluent discharge using an online charge analyzing system titrator (CAST). *J. Ind. Eng. Chem.* 21, 269–277.
- Li, M., Liu, J., Xu, Y., Qian, G., Li, M., Xu, Y., 2016. Phosphate adsorption on metal oxides and metal hydroxides: a comparative review. *Environ. Rev.* 24, 1–58.
- Lin, J., Zhan, Y., Wang, H., Chu, M., Wang, C., He, Y., Wang, X., 2016. Effect of calcium ion on phosphate adsorption onto hydrous zirconium oxide. *Chem. Eng. J.* 309, 118–129.
- Lingamdinne, L., Koduru, J., Karri, R., 2019. A comprehensive review of applications of magnetic graphene oxide based nanocomposites for sustainable water purification. *J. Environ. Manag.* 231, 622–634.
- Liu, A.R., Chi, L., Wang, X., Sui, Y., 2018. Review of metal (Hydr)oxide and other adsorptive materials for phosphate removal from water. *J. Environ. Chem. Eng.* 6, 5269–5286.
- Liu, J., Wan, L., Zhang, L., Zhou, Q., 2011. Effect of pH, ionic strength, and temperature on the phosphate adsorption onto lanthanum-doped activated carbon fiber. *J. Colloid Interface Sci.* 364, 490–496.
- Liu, J., Zhou, Q., Chen, J., Zhang, L., Chang, N., 2013. Phosphate adsorption on hydroxyl-iron-lanthanum doped activated carbon fiber. *Chem. Eng. J.* 216, 859–867.
- Liu, X., Zong, E., Hu, W., Song, P., Wang, J., Liu, Q., Fu, S., 2019. Lignin-derived porous carbon loaded with La(OH)<sub>3</sub> nanorods for highly efficient removal of phosphate. *ACS Sustain. Chem. Eng.* 7, 758–768.
- Loganathan, P., Vigneswaran, S., Kandasamy, J., Nanthi, B., 2014. Removal and recovery of phosphate from water using sorption. *Crit. Rev. Environ. Sci. Technol.* 44, 847–907.
- Luo, X., Wang, X., Bao, S., Liu, X., Zhang, W., Fang, T., 2016. Adsorption of phosphate in water using one-step synthesised zirconium-loaded reduced graphene oxide. *Sci. Rep.* 6, 1–13.
- Mahardika, D., Park, H., Choo, K., 2018. Ferrihydrite-impregnated granular activated carbon (FH@GAC) for efficient phosphorus removal from wastewater secondary effluent. *Chemosphere* 207, 527–533.
- Mahdavi, S., Akhbari, D., 2016. The removal of phosphate from aqueous solutions using two nano-structures: copper oxide and carbon tubes. *Clean Technol. Environ. Policy* 18, 817–827.
- Makita, Y., Sonoda, A., Sugiura, Y., Ogata, A., Suh, C., Lee, J., 2019. Preparation and phosphate adsorptive properties of metal oxide-loaded granular activated carbon and pumice stone. *Colloids Surfaces A Physicochem. Eng. Asp.* 582, 123881.
- Manjunath, S.V., Kumar, M., 2018. Evaluation of single-component and multi-component adsorption of metronidazole, phosphate and nitrate on activated carbon from *Prosopis juliflora*. *Chem. Eng. J.* 346, 525–534.
- Mashkoor, F., Nasar, A., 2020. Carbon nanotube-based adsorbents for the removal of dyes from waters: a review. *Environ. Chem. Lett.* 18, 605–629.
- Mehrabi, N., Soleimani, M., Sharififard, H., Yeganeh, M.M., 2016. Optimization of phosphate removal from drinking water with activated carbon using response surface methodology (RSM). *Desalin. Water Treat.* 57, 15613–15618.
- Minale, M., Gu, Z., Guadie, A., Manaye, D., Li, Y., 2020. Application of graphene-based materials for removal of tetracyclines using adsorption and photocatalytic-degradation: a review. *J. Environ. Manag.* 276, 111310.
- Mor, S., Chhoden, K., Negi, P., Ravindra, K., 2017. Utilization of nano-alumina and activated charcoal for phosphate removal from wastewater. *Environ. Nanotechnology, Monit. Manag.* 7, 15–23.
- Nakarmi, A., Bourdo, S.E., Ruhl, L., Kanel, S., Nadagouda, M., Kumar, P., Pavel, I., Viswanathan, T., 2020. Benign zinc oxide betaine-modified biochar nanocomposites for phosphate removal from aqueous solutions. *J. Environ. Manag.* 272, 111048.
- Namasivayam, C., Sangeetha, D., 2004. Equilibrium and kinetic studies of adsorption of phosphate onto ZnCl<sub>2</sub> activated coir pith carbon. *J. Colloid Interface Sci.* 280, 359–365.
- Nodeh, H.R., Sereshti, H., Afsharian, E.Z., Nouri, N., 2017. Enhanced removal of phosphate and nitrate ions from aqueous media using nanosized lanthanum hydrous doped on magnetic graphene nanocomposite. *J. Environ. Manag.* 197, 265–274.
- Novais, S., Delgado, M., Zenero, O., Tronto, J., Feola, R., Eduardo, C., Cerri, P., 2018. Poultry manure and sugarcane straw biochars modified with MgCl<sub>2</sub> for phosphorus adsorption. *J. Environ. Manag.* 214, 36–44.
- Ouakouak, A., Youcef, L., Boulanour, D., Achour, S., 2017. Adsorptive removal of phosphate from groundwater using granular activated carbon. *Int. J. Eng. Res. Afr.* 32, 53–61.
- Qi, X., Li, L., Wang, Y., Liu, N., Smith, R.L., 2014. Removal of hydrophilic ionic liquids from aqueous solutions by adsorption onto high surface area oxygenated carbonaceous material. *Chem. Eng. J.* 256, 407–414.
- Quimpo, T.J.R., Ligson, C.A., Manogan, D.P., Requielme, J.N.C., Albelda, R.L., Conaco, C., Cabaitan, P.C., 2020. Fish farm effluents alter reef benthic assemblages and reduce coral settlement. *Mar. Pollut. Bull.* 153, 111025.
- Sakamoto, T., Amano, Y., Machida, M., 2020. Phosphate ion adsorption properties of PAN-based activated carbon fibers prepared with K<sub>2</sub>CO<sub>3</sub> activation. *SN Appl. Sci.* 2, 1–8.
- Sakulpaisan, S., Vongsetskul, T., Reamouppattum, S., Jakkrawut, L., Jonggol, T., Pramuan, T., 2016. Titania-functionalised graphene oxide for an efficient adsorptive removal of phosphate ions. *J. Environ. Manag.* 167, 99–104.
- Shi, Z., Liu, F., Yao, S., 2011. Adsorptive removal of phosphate from aqueous solutions using activated carbon loaded with Fe(III) oxide. *N. Carbon Mater.* 26, 299–306.
- Siyal, A., Rashid, M., Low, A., Ekmi, N., 2020. A review on recent developments in the adsorption of surfactants from wastewater. *J. Environ. Manag.* 254, 109797.
- Smith, S.C., Rodrigues, D.F., 2015. Carbon-based nanomaterials for removal of chemical and biological contaminants from water: a review of mechanisms and applications. *Carbon N. Y.* 91, 122–143.
- Suresh, S., Bandosz, T.J., 2018. Removal of formaldehyde on carbon-based materials: a review of the recent approaches and findings. *Carbon N. Y.* 137, 207–221.
- Tran, D., Kabiri, S., Wang, L., Losic, D., 2015. Engineered graphene-nanoparticle aerogel composites for efficient removal of phosphate from water. *J. Mater. Chem.* 3, 6844–6852.
- Vasudevan, S., Lakshmi, J., 2012. The adsorption of phosphate by graphene from aqueous solution. *RSC Adv.* 2, 5234–5242.
- Vikrant, K., Kim, K., Sik, Y., Tsang, D.C.W., Fai, Y., Shekhar, B., Sharan, R., 2017. Engineered/designer biochar for the removal of phosphate in water and wastewater. *Sci. Total Environ.* 616–617, 1242–1260.
- Wang, Y., Yang, Q., Huang, H., 2019. Effective adsorption of trace phosphate and aluminum in realistic water by carbon nanotubes and reduced graphene oxides. *Sci. Total Environ.* 662, 1003–1011.
- Wang, Z., Nie, E., Li, J., Yang, M., 2012. Equilibrium and kinetics of adsorption of phosphate onto iron-doped activated carbon. *Environ. Sci. Pollut. Res.* 19, 2908–2917.
- Wang, Z., Shi, M., Li, J., Zheng, Z., 2014. Influence of moderate pre-oxidation treatment on the physical, chemical and phosphate adsorption properties of iron-containing activated carbon. *J. Environ. Sci.* 26, 519–528.
- Xiang, Y., Xu, Z., Wei, Y., Zhou, Y., Yang, X., Yang, Y., 2019. Carbon-based materials as adsorbent for antibiotics removal: mechanisms and influencing factors. *J. Environ. Manag.* 237, 128–138.
- Xiong, W., Tong, J., Yang, Z., Zeng, G., Zhou, Y., Wang, D., 2017. Adsorption of phosphate from aqueous solution using iron-zirconium modified activated carbon nanofiber: performance and mechanism. *J. Colloid Interface Sci.* 493, 17–23.
- Xiong, W., Zeng, G., Yang, Z., Zhou, Y., Zhang, C., Cheng, M., Liu, Y., Hu, L., Wan, J., Zhou, C., Xu, R., Li, X., 2018. Adsorption of tetracycline antibiotics from aqueous solutions on nanocomposite multi-walled carbon nanotube functionalised MIL-53 (Fe) as new adsorbent. *Sci. Total Environ.* 627, 235–244.
- Xu, H., Hu, J., Ren, X., Li, G., 2016. Macroscopic and microscopic insight into the mutual effects of europium (III) and phosphate on their interaction with graphene oxide. *RSC Adv.* 6, 85046–85057.
- Xu, X., Song, W., Huang, D., Gao, B., Sun, Y., Yue, Q., Fu, K., 2015. Performance of novel biopolymer-based activated carbon and resin on phosphate elimination from stream. *Colloids Surfaces A Physicochem. Eng. Asp.* 68–75.
- Yagub, M.T., Sen, T.K., Afroz, S., Ang, H.M., 2014. Dye and its removal from aqueous solution by adsorption: a review. *Adv. Colloid Interface Sci.* 209, 172–184.
- Yang, Y., Wang, J., Qian, X., Shan, Y., Zhang, H., 2018. Aminopropyl-functionalised mesoporous carbon (APTMS-CMK-3) as effective phosphate adsorbent. *Appl. Surf. Sci.* 428, 206–214.
- Yao, S., Wang, M., Liu, J., Tang, S., Chen, H., 2018. Removal of phosphate from aqueous solution by sewage sludge-based activated carbon loaded with pyrolusite. *J. Water Reuse Desalin.* 8, 192–201.

- Yuan, J., Hu, M., Zhou, Z., Wang, L., 2014. Kinetic and thermodynamic behavior of the batch adsorption of phosphate from aqueous solutions onto environmentally friendly barbecue bamboo charcoal. *Desalin. Water Treat.* 52, 7248–7257.
- Yuan, K., Zhao, R., Zheng, J., Zheng, H., Nagase, S., 2017. Van Der Waals heterogeneous layer-layer carbon nanostructures involving  $\pi$ -H-C-C-H- $\pi$ -H-C-C-H stacking based on graphene and graphane sheets. *J. Comput. Chem.* 38, 730–739.
- Zach-maor, A., Semiat, R., Shemer, H., 2011. Synthesis, performance, and modeling of immobilized nano-sized magnetite layer for phosphate removal. *J. Colloid Interface Sci.* 357, 440–446.
- Zare, K., Gupta, V.K., Moradi et al, O., 2015. A comparative study on the basis of adsorption capacity between CNTs and activated carbon as adsorbents for removal of noxious synthetic dyes: a review. *J. Nanostructure Chem.* 5, 227–236.
- Zhang, L., Gao, Y., Li, M., Liu, J., 2015. Expanded graphite loaded with lanthanum oxide used as a novel adsorbent for phosphate removal from water: performance and mechanism study. *Environ. Technol.* 36, 1016–1025.
- Zhang, L., Gao, Y., Zhou, Q., Kan, J., Wang, Y., 2014. High-performance removal of phosphate from water by graphene nanosheets supported lanthanum hydroxide nanoparticles. *Water, Air, Soil Pollut.* 225, 1967.
- Zhang, L., Li, M., Gao, Y., Liu, J., Xu, Y., 2016a. Performance and mechanism study on phosphate adsorption onto activated carbon fiber loading lanthanum and iron oxides. *Desalin. Water Treat.* 57, 37–41.
- Zhang, L., Liu, J., Lihua, W., Qi, Z., Wang, X., 2012a. Batch and fixed-bed column performance of phosphate adsorption by lanthanum-doped activated carbon fiber. *Water, Air, Soil Pollut.* 223, 5893–5902.
- Zhang, L., Wan, L., Chang, N., Liu, J., Duan, C., Zhou, Q., Li, X., Wang, X., 2011. Removal of phosphate from water by activated carbon fiber loaded with lanthanum oxide. *J. Hazard Mater.* 190, 848–855.
- Zhang, L., Zhou, Q., Liu, J., Chang, N., Wan, L., Chen, J., 2012b. Phosphate adsorption on lanthanum hydroxide-doped activated carbon fiber. *Chem. Eng. J.* 185–186, 160–167.
- Zhang, X., Wei, W., Wenxin, S., Jiaojie, H., Hui, F., Yongpeng, X., Fuyi, C., Ce, W., 2016b. LaCO<sub>3</sub>OH embedded in carbon nanofiber matrix synchronously as capturer of phosphate and organic carbon for starving Bacteria. *J. Mater. Chem.* 4, 12799–12806.
- Zhang, Y., Guo, X., Yao, Y., Wu, F., Zhang, C., Chen, R., 2016c. Mg-enriched engineered carbon from lithium-ion battery anode for phosphate removal. *ACS Appl. Mater. Interfaces* 8, 2905–2909.
- Zhang, Y., Guo, X., Yao, Y., Wu, F., Zhang, C., Lu, J., 2016d. Synthesis of Mg-decorated carbon nanocomposites from MesoCarbon MicroBeads (MCMB) graphite: application for wastewater treatment. *ACS Omega* 1, 417–423.
- Zhao, J., Wang, Z., White, J.C., Xing, B., 2014. Graphene in the aquatic environment: adsorption, dispersion, toxicity and transformation. *Environ. Sci. Technol.* 48, 9995–10009.
- Zhi, Y., Zhang, C., Hjorth, R., Baun, A., Duckworth, O.W., Call, D.F., Knappe, D.R.U., Jones, J.L., Grieger, K., 2020. Emerging lanthanum (III)-containing materials for phosphate removal from water: a review towards future developments. *Environ. Int.* 145, 106115.
- Zhou, Q., Wang, X., Liu, J., Zhang, L., 2012. Phosphorus removal from wastewater using nano-particulates of hydrated ferric oxide doped activated carbon fiber prepared by Sol-Gel method. *Chem. Eng. J.* 200–202, 619–626.
- Zhu, X., Yuchen, L., Feng, Q., Hua, S., Xinchao, W., Shicheng, Z., Chen, J., Zhiyong, J.R., 2018. Carbon transmission of CO<sub>2</sub> activated nano-MgO carbon composites enhances phosphate immobilization. *J. Mater. Chem.* 6, 3705–3713.
- Zong, E., Liu, X., Wang, J., Yang, S., Jiang, J., Fu, S., 2017. Facile preparation and characterization of lanthanum-loaded carboxylated multi-walled carbon nanotubes and their application for the adsorption of phosphate ions. *J. Mater. Sci.* 52, 7294–7310.
- Zong, E., Wei, D., Wan, H., Zheng, S., Xu, Z., Zhu, D., 2013. Adsorptive removal of phosphate ions from aqueous solution using zirconia-functionalised graphite oxide. *Chem. Eng. J.* 221, 193–203.